Food and Bioprocess Technology (2024) 17:4960–4979
https://doi.org/10.1007/s11947-024-03410-3

RESEARCH

Obtaining Extracts and Hydrolysates from Cambuci Peel Through Subcritical Water: An In-line Detection Approach

Juver Andrey Jimenez Moreno[1] · Leonardo de Freitas Marinho[1] · Letícia Sanches Contieri[2] · Tiago Linhares Cruz Tabosa Barroso[1] · Mauricio Ariel Rostagno[2] · Tânia Forster Carneiro[1]

Received: 7 December 2023 / Accepted: 16 April 2024 / Published online: 7 May 2024

Abstract

The cambuci is a fruit that has been attracting interest due to its rich composition of phenolic compounds. However, the fruit's peel is an understudied agro-industrial by-product. This study is aimed at assessing the effects of temperature and pH in an innovative system. This system integrates an in-line UV-VIS analysis detector into the process of extracting and hydrolyzing bioactive compounds from cambuci peel, enhancing process monitoring. The system operated with 2 g of cambuci peel in the reactor for 60 min, using a water flow rate of 2 mL min^{-1}, 15 MPa, temperatures ranging from 40 to 160 °C, and pH levels from 4 to 7. The results indicated that increasing the temperature led to a more favorable response in total phenolic compounds (TPC) and the antioxidant capacity of the samples. At the same time, the selected pH range had a minimal impact. Furthermore, the obtained material revealed the presence of citric acid, glucose, arabinose, and fructose, with fructose showing the highest concentration. The in-line coupling system proved to be highly effective in real-time monitoring and determining the completion of the extraction or hydrolysis process, as it allowed for the observation of decreasing concentrations of the compounds of interest. Thus, this study contributes to the understanding and optimization of the extraction of bioactive compounds from cambuci peel, providing valuable insights for future applications in the food and natural products industry.

Keywords Bioactive compounds · Biomass · Biorefinery · Circular economy · Hydrolysis

Introduction

Brazil is one of the world's most biodiverse nations, boasting an astounding array of over 40,000 distinct plant species, constituting an impressive 20% of the Earth's plant life (Oliveira et al., 2012). Nonetheless, numerous native and exotic species remain relatively untapped but can serve as a revenue source for the local community. Furthermore, it presents an opportunity to enter niche markets where consumers seek compounds known for their health benefits (Seraglio et al., 2018). The *Myrtaceae* family comprises approximately 145 genera and 5970 species (Barbieri et al., 2017), ranking as one of the prominent families within the Brazilian Atlantic Forest (Stefanello et al., 2011). Nonetheless, several fruits within this family are still classified as wild plants or are traded at a limited scale (Donado-Pestana et al., 2015). Among them are the camu-camu (*M. dubia* McVaugh), the guabiju, the jambolan (*S. cumini* (L.) Skeels), and the cambuci (*Campomanesia phaea* O. Berg) (Donado-Pestana et al., 2015; Seraglio et al., 2018).

Cambuci is found mainly in Minas Gerais State, São Paulo (SP) State, and Rio de Janeiro (RJ) State of Brazil. The fruit has a diameter of 5–6 cm, high humidity, acidity, and fiber content (Donado-Pestana et al., 2018). In addition, it is made up of approximately 80.5% pulp, 18.5% peel, and 1% seeds (Tokairin et al., 2018). The annual production of this fruit can reach 300 tons (Donado-Pestana et al., 2015). Certain studies have indicated that cambuci is rich in polyphenolic compounds, including ellagitannins and proanthocyanidins (Paes et al., 2021; Sanches Azevedo et al., 2017), and a high antioxidant capacity in vitro (Sanches Azevedo et al., 2017). The peel becomes the main by-product throughout the processing and represents an approximate waste of

✉ Mauricio Ariel Rostagno
mauricio.rostagno@fca.unicamp.br

✉ Tânia Forster Carneiro
taniafc@unicamp.br

[1] School of Food Engineering, University of Campinas (UNICAMP), 13083-862 Campinas, SP, Brazil

[2] School of Applied Sciences (FCA), University of Campinas (UNICAMP), 13484-350 Limeira, SP, Brazil

55.5 tons per year. Information on the use of cambuci peel is limited because this fruit lacks a large-scale industry. However, the company Asmussen (Natividade da Serra, SP, Brazil) has reported that some of the by-products are destined for composting. On the other hand, Souza Ronchi (2021) mentions that cambuci peel is used to make tea, representing a potential market opportunity. This by-product remains largely unexplored but could be a source of polyphenolic compounds and sugars of interest to the food industry.

Recently, there has been growing interest in a more sustainable economy, with the concept of a circular economy gaining significance. Its primary goal is the reduction and reuse of by-products (Grimaldi et al., 2022). Some research has been carried out on the use of by-products in different areas, including animal feed (Murugesan et al., 2021; Rahmani et al., 2022), material processing Grimaldi et al., 2022), industrial chemical products (Arslan et al., 2016), and energy (Chen et al., 2023), which allows establishing that by-products should continue to be studied, especially by their applications in the industry. Besides, over the last 5 decades, environmentally friendly extraction techniques have been developed to minimize the use of organic and synthetic chemicals, shorten extraction times, and enhance the yield and quality of extracts (Jha & Sit, 2022). The extraction of bioactive compounds from these by-products often involves the use of solvents such as methanol, ethanol, water, acetone, and, in some cases, acidified water (Bunmusik et al., 2022; Chanioti & Tzia, 2018; Cvjetko Bubalo et al., 2016; Kumar et al., 2021). For a sustainable bioactive compound extraction process, the use of "green" extraction methods is essential (Osamede Airouyuwa et al., 2022). These methods are considered safe and sustainable once proven to eliminate toxic solvents, reduce energy consumption, and reduce environmental impact (Barba et al., 2015; Osamede Airouyuwa et al., 2022).

Hydrothermal pretreatment (HTP) under high-pressure conditions becomes a sustainable alternative for the extraction and hydrolysis process. This is because water in a sub/supercritical state has low viscosity and high diffusivity, making it easier to penetrate the structure of the lignocellulosic matrix. Furthermore, the low dielectric constant of supercritical water enhances the solubility of organic compounds (Maciel-Silva et al., 2019). The manipulation of temperature and pressure conditions allows for adjustments to the physical properties of water, including density, ionic product, and dielectric constant (Cocero et al., 2018).

Coupling an in-line detector to the extraction and hydrolysis process in subcritical water is a combination of technologies that allows real-time analysis of the extracted components. However, a detailed analysis of samples in an innovative subcritical water extraction system with in-line detection is necessary to confirm the benefits of this combination. The hydrothermal treatment of cambuci peel is a promising option for exploring compounds with potential value in the cosmetic, pharmaceutical, and food industries. Moreover, employing water as an extraction solvent facilitates an eco-friendly and cost-effective process, given its short extraction times and high efficiency (Zhang et al., 2020). Additionally, it enables the comprehensive utilization of the entire product, thereby minimizing waste generation and mitigating potential negative environmental impacts.

To achieve this, it is crucial to characterize the extracts and hydrolysates obtained from the system, enabling future applications to be envisioned. The study aims to characterize the extracts and hydrolysates of the cambuci peel obtained through subcritical water in an in-line detection system, varying the temperature and pH.

Materials and Methods

Raw Material

The cambuci peel, provided by the Asmussen Company (Natividade da Serra, SP, Brazil), was dried at 60 °C for 24 h, crushed into 1 mm particles after drying, and stored at − 18 °C for physicochemical characterization and obtaining the extracts. The analysis included total solids, volatile solids, moisture, ashes, total protein, and total nitrogen AOAC (2012), and the elementary analysis was conducted (CHNS-O element analyzer, Thermo Fisher Scientific Inc., The Netherlands).

System of Coupling a Detector Analysis In-line on Subcritical Water Process

The extraction and hydrolysis in subcritical water were carried out using a semi-continuous flow reactor with a total volume of 100 mL (Fig. 1). The system came equipped with a high-pressure liquid pump featuring a double piston (Model 36-USA), which fed and pressurized the system. A micrometric valve was employed to control the system pressure and was measured with manometers (0–50 MPa). The extraction and hydrolysis temperature were monitored with two thermocouples (type K) inside and outside the reactor. The hydrolysates were cooled using a coil submerged in a thermostatic bath (Marconi, model MA-184, São Paulo, SP, Brazil), which used water as a coolant at 10 °C.

The reactor operating conditions and process variables (temperature and pH) were determined based on information obtained in previous studies (Barroso et al., 2022a, b; Ferreira et al., 2023; Lachos-Perez et al., 2020; Maciel-Silva et al., 2019; Sganzerla et al., 2022). For the hydrothermal pretreatment, the system was operated for 60 min with a feed of 2 g of dry cambuci peel at a constant pressure and flow of 15 MPa and 2 mL min^{-1}. Samples were collected at 6-min intervals to ascertain the kinetics of extraction and hydrolysis. Then, the extracts

(a)

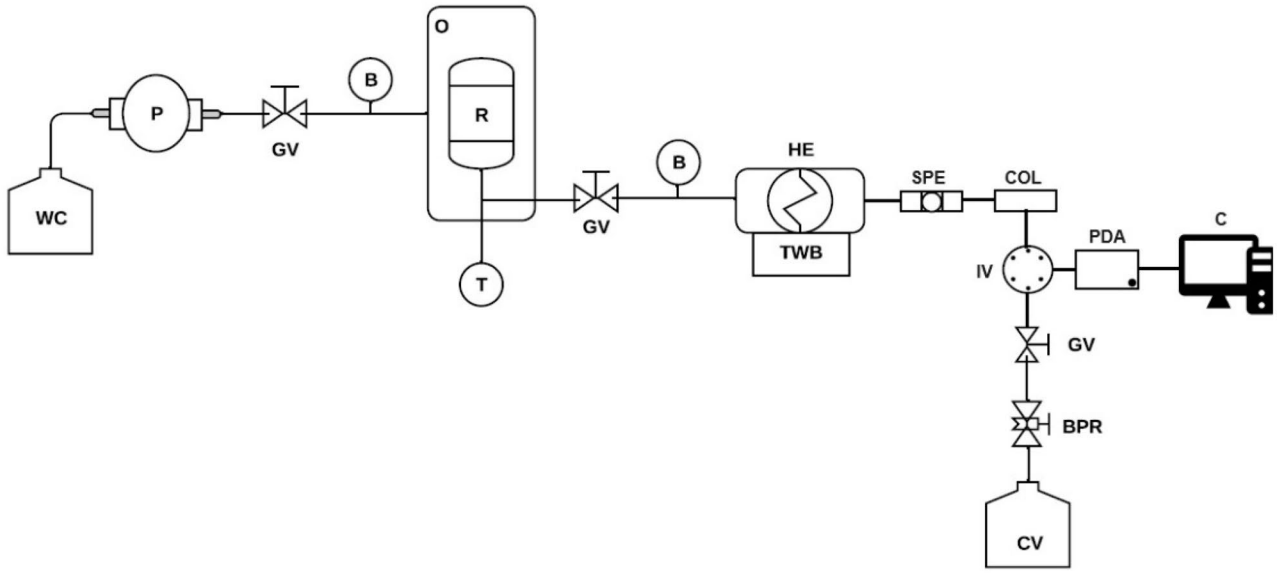

(b)

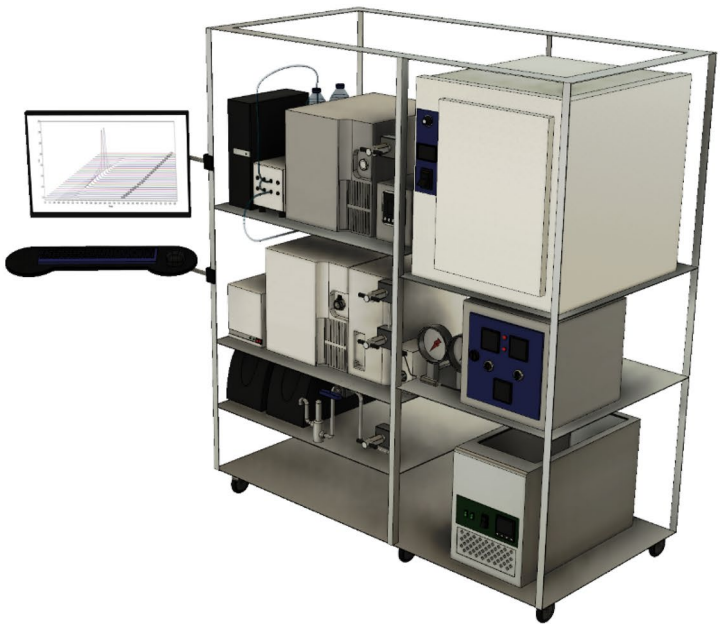

Fig. 1 Experimental unit for extraction and hydrolysis of cambuci peel. **a** Schematic diagram; **b** 3D representation. Label: WC, water container; P, pump; GV, gate valve; HE, heat exchanger; B, barometer; O, oven; R, reactor; T, thermostat; TWB, thermostatic water bath; SPE, solid phase extraction; COL, column; IV, interface valve; PDA, detector; C, computer; BPR, micrometric valve; CV, collect vessel

and hydrolysates were centrifuged at 3000 rpm for 10 min and stored at − 18 °C for future analysis. The hydrothermal process of the cambuci peel was performed using the surface response methodology (RSM). It involved the utilization of central composite rotatable design (CCDR), for two independent variables (temperature and pH). The best extraction/hydrolysis condition will be selected for monitoring in an in-line system (PLE-PDA). It utilizes pressurized liquid extraction (PLE) with detection in-line employing a photodiode array (PDA). The temperatures of 40 and 57 °C will be considered extraction temperatures, and temperatures of 100, 143, and 160 °C will be considered hydrolysis temperatures (Table 1).

Extract and Hydrolysate Characterization

Color

The colorimetric coordinates L^* (lightness), a^* (red/green value), and b^* (blue/yellow value) of the CIELab system were obtained by measuring transmittance values every 5 nm between 340 and 830 nm in a UV-Vis spectrophotometer (Model UV-M51, Bell Photonics) (Gilchrist & Nobbs, 2017; Ohta & Robertson, 2006). The hue angle ($h°$) was calculated using Formula 1.

$$h° = \tan^{-1}\left(\frac{b^*}{a^*}\right) \quad (1)$$

pH

The pH was measured using a digital pH meter (model THS-3E- USA) at 25 °C. The pH meter was previously calibrated with buffer solutions.

Antioxidant Activity Through Free Radical DPPH and FRAP Assays

The antioxidant capacity of the cambuci peel extracts and hydrolysates was assessed by measuring their ability to inhibit the 2,2-diphenyl-1-picrylhydrazyl (DPPH) free radical (da Silveira et al., 2018). In this assay, 150 µL of the sample was mixed with a 5.85 mL DPPH solution and incubated in the dark for 30 min. After, the absorbance at 515 nm was determined using a UV-Vis spectrophotometer (Model UV-M51, Bell Photonics). A Trolox standard curve (50–1000 µM) was used for quantification ($y = -0.0006x + 0.6762$, $R^2 = 0.9922$). The analysis was carried out in triplicate ($n = 3$). The results were expressed as µmol of Trolox equivalent antioxidant capacity (TEAC) g^{-1} dry cambuci peel (µmol g^{-1}).

The ferric reducing antioxidant power (FRAP) assay, modified from the procedure outlined by Benzie and Strain (1996), comprised the combination of 200 µL of the sample with 200 µL of a 3 mM ferric chloride solution and 3.6 mL of a 2,4,6-Tris(2-Pyridyl)-S-Triazine (TPTZ) solution. This mixture underwent incubation at 37 °C for a duration of 30 min, followed by 10 min of rest in a lightless setting. Subsequently, the absorbance at 620 nm was measured in a UV-Vis spectrophotometer (Model UV-M51, Bell Photonics). A Trolox calibration curve (100–1000 µM) was used for quantification ($y = 0.0018x + 0.0319$, $R^2 = 0.9976$). The analysis was conducted in triplicate ($n = 3$). The results were expressed as µmol of Trolox equivalent antioxidant capacity (TEAC) g^{-1} dry cambuci peel (µmol g^{-1}).

Total Phenolic Compounds

TPC was measured using the Folin–Ciocalteu method (Singleton et al., 1999) with modifications. Added 60 µL of samples to a mixture containing 300 µL of Folin–Ciocalteu reagent and 3 mL of distilled water. The solution was homogenized, and after 3 min in the dark environment, 0.9 mL of sodium carbonate (15%) and 1.74 mL of distilled water were added. After 2 h, the absorbance at 765 nm was determined using a UV-Vis spectrophotometer (Model UV-M51, Bell Photonics). The values were determined based on a calibration curve (0–1000 µM) using a gallic acid solution ($y = 0.0005x - 0.0127$, $R^2 = 0.9935$). The results were reported in mg gallic acid equivalent (GAE) g^{-1} dry cambuci peel.

Table 1 Model's experimental parameters and test responses

Test		Non-codified variables		Codified variables		DPPH (µmol TEAC g^{-1})	FRAP (µmol TEAC g^{-1})	Reducing sugar (mg g^{-1})	TPC (mg g^{-1})
		Temperature (°C)	pH	Temperature (°C)	pH				
T1	Extraction	57	4.4	–1	–1	58.30	96.15	104.65	10.55
T2	Hydrolysis	143	4.4	+1	–1	56.36	456.57	105.86	45.91
T3	Extraction	57	6.6	–1	+1	57.21	85.70	87.48	10.35
T4	Hydrolysis	143	6.6	+1	+1	52.14	302.29	132.54	38.57
T5	Extraction	40	5.5	–1.41	0	55.80	66.34	85.63	6.72
T6	Hydrolysis	160	5.5	+1.41	0	47.22	501.91	101.59	46.40
T7	Hydrolysis	100	4.0	0	–1.41	61.41	149.55	120.75	17.79
T8	Hydrolysis	100	7.0	0	+1.41	56.69	156.18	53.15	15.89
T9	Hydrolysis	100	5.5	0	0	58.91	165.74	116.01	16.75
T10	Hydrolysis	100	5.5	0	0	58.20	165.35	115.99	15.77
T11	Hydrolysis	100	5.5	0	0	57.45	163.71	114.98	16.24

Reducing Sugars

The concentration of reducing sugars (RS) was assessed through a Somogyi–Nelson Method, described by Norton (1944). The absorbance of the reaction was determined at 540 nm using a UV-Vis spectrophotometer (Model UV-M51, Bell Photonics). A calibration curve of glucose was used for quantification (50–500 mg L^{-1}) ($y = 5000.36x - 41.108$, $R^2 = 0.9862$). The analysis was performed in triplicate ($n = 3$), and the results were reported as mg glucose g^{-1} dry peel of cambuci.

Sugars, Citric Acid, and Inhibitors

Sugars, citric acid, and inhibitors were quantified utilizing HPLC coupled with a refractive index detector (RID), following the procedure described by Barroso et al. (2022a, b). Concentrations of glucose, fructose, arabinose, citric acid, and 5-HMF were computed based on calibration curves for each corresponding standard. The results were reported as mg g^{-1} of dried cambuci peel.

UPLC-PDA-MS Analysis

After establishing optimal conditions, the cambuci peel extracts were diluted fivefold in water, filtered in a nylon filter of 0.22 µm, and further injected in an ultra-performance liquid chromatography coupled to a photodiode array and mass spectrometry (UPLC-PDA-MS) (Acquity, Waters Co., Milford, MA, USA). The separation system was performed in an Acquity UPLC BEH C18 50 × 2.1 mm, 1.7 µm analytical column, and the mobile phases consisted of water (A) and acetonitrile (B), both acidified with 0.1% acetic acid (v/v). The gradient elution was 2% B (0–1 min), 2–15% B (1–2 min), 15–35% B (2–8 min), 35–100% B (8–10 min), and 100% B (10–12 min). The chromatography conditions were a flow rate of 0.5 mL/min, a column oven at 40 °C, and an injection volume of 3 µL. UV spectra were recorded from 210 to 400 nm at λmax of 254 nm. MS analysis was performed in positive and negative ionization mode (100–1000 Da) with cone voltage of 15 V and 30 V, respectively, capillary voltage of 0.8 kV, and probe at 600 °C. The software Empower 3 was applied for data processing (Waters Alliance, Milford, MA, USA). The term "fraction" denotes the specific time intervals during extraction. For instance, fraction 1 corresponds to the initial 6 min, fraction 2 to 12 min, and so forth, with fraction 10 representing the entire 60-min extraction period.

Statistical Analysis

The results were subjected to statistical analysis using one-way analysis of variance (ANOVA), and significant differences at the 5% level were further assessed through Tukey's test. Statistical analysis was conducted using Statistica® software (version 10.0, StatSoft Inc., OK, USA). The experimental results for antioxidant activity, phenolic compounds, reducing sugars, and organic acids were analyzed by response surface methodology (RSM).

Results and Discussion

Evaluation of Raw Material

The composition of dried cambuci peel is presented in Table 2. The value obtained for the moisture of the cambuci peel was 7.36 ± 0.11%. The protein results (4.93 ± 0.04%) are higher than those reported by Sanches Azevedo et al. (2017) for the cambuci pulp (2.09 ± 0.01%) and even higher than those reported by Damiani et al. (2011) for araça peel (1.39 ± 0.76%), a fruit that also belongs to the *Myrtaceae* family. On the other hand, the ash content of the cambuci peel is higher than those reported by Schiassi et al. (2018) for the araça and cagaita pulp (belonging to the *Myrtaceae* family). However, the ashes obtained from the cambuci peel (1.23 ± 0.11%) turn out to be approximately 50% of that obtained in the pulp of this fruit, as reported by Sanches Azevedo et al. (2017) and Sanches (2013). Elementary analysis shows that the cambuci peel is composed mainly of oxygen (48.70%) and carbon (44.38%) and to a lesser extent, hydrogen (5.93%) and nitrogen (1.00%), values close to those reported by Rojas-González et al. (2019) for by-products such as passion fruit peel, soursop peel, and pineapple peel.

Table 2 Composition of dried cambuci peel

Parameters	Cambuci peel
Total solids (%)	92.64 ± 0.11
Volatile solids (%)	91.41 ± 0.01
Moisture (%)	7.36 ± 0.11
Total protein (%)	4.93 ± 0.04
Total nitrogen (%)	0.79 ± 0.01
Elementary analysis	
Ashes (%)	1.23 ± 0.11
Nitrogen (%)	1.00
Carbon (%)	44.38
Hydrogen (%)	5.93
Sulfur (%)	0
Oxygen (%)	48.70

The results are presented as the mean ± standard deviation
The analysis was performed in triplicate ($n = 3$)

Color

Figure 2 presents the color of extracts and hydrolysates for 11 tests. The extract obtained at 40 °C (T5) had a lower color intensity during all the collection times. Likewise, at 57 °C (T1 and T3), the extracts show less color intensity in the first 12 min, increasing after up to minute 48. Later, intensity decreases, possibly due to extraction process completion (Ferreira et al., 2023). At 100 °C (T7-T11), between 12 and 24 min, slight darkening appears in extracts. On the other hand, the tests at 143 and 160 °C (T2, T4, and T6) show significant color change, becoming darker and browner. This can be attributed to Maillard reaction products and sugar decomposition products, also called caramelization products, which are directly related to the high temperatures of the process (Agcam, 2022). Similar results have been observed in extracts and hydrolysates of jaboticaba peel (Barroso et al., 2022a, b), pitaya peel (Ferreira et al., 2023), and açai seeds (Maciel-Silva et al., 2019).

Table 3 presents the CIELab color appearance parameters ($h°$, b^*, L^*, and a^*) of the extracts and hydrolysates post-hydrothermal pretreatment. For the extracts that were obtained at low temperatures (40 and 57 °C), the luminosity values (L^*) ranged between 74.68 and 98.04, which indicates that the coloration of the extract is closer to white (Yee et al., 2023). For the tests carried out at 100 °C, the values of L^* oscillated between 30.27 and 95.86, which allows for determining a greater variation in the luminosity of the extracts with increasing temperature. Likewise, significant differences were found between the collection times of hydrolysates at 100 °C. The hydrolysates at temperatures of 143 and 160 °C presented an oscillation between 0.08 and 97.42 for this parameter, with significant differences for all collection times. However, it was possible to establish that the values closest to 0.08 were found at 12 and 18 min and gradually increased to 60 min.

For the parameter a^* (greenness (−) to redness (+)), extraction temperatures yielded the lowest values (40 and 57 °C), varying between − 0.48 and 1.18. Furthermore, extraction at 40 °C showed no significant differences in any sampling times by the Tukey test. For hydrolysis at 143 °C and pH 4.4, the maximum value was obtained at 36 min ($a^* = 29.01$). In the case of hydrolysis at 143 °C and pH 6.6 and hydrolysis at 160 °C, the highest values of a^* parameter were 27.82 and 36.56, respectively, and were found at 30 min. As expected, the highest values for the a^* parameter were found in the samples subjected to higher temperatures, which could induce oxidation of the phenolics present in the extracts and generate a reddish color (He et al., 2019; Yao et al., 2023). The highest a^* values for hydrolysates at 100 °C were achieved between 18 and 24 min during the hydrothermal process.

Analyzing the b^* parameter, it is evident that the extraction temperatures displayed lower values, ranging from 1.98 to 10.87. Regarding hydrolysis temperature, the peak value ($b^* = 58.28$) occurred at 160 °C, precisely at 42 min into the process. Based on the above, it can be concluded that higher temperatures promote the extraction of water-soluble

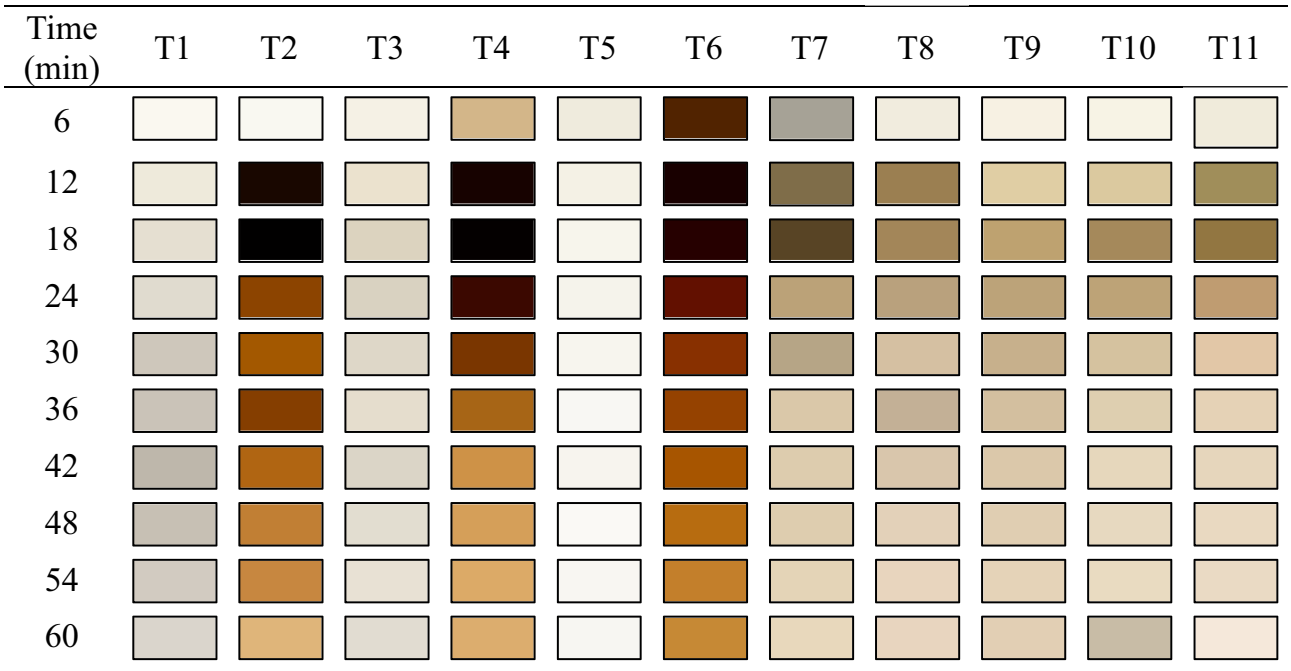

Fig. 2 Visual depiction of the color of the extracts and hydrolysates acquired from the cambuci peel

Table 3 Color parameters of the samples obtained from the cambuci peel through hydrothermal processing

Parameters	T1	T2	T3	T4	T5	T6	T7	T8	T9	T10	T11
*L**											
6 min	97.45 ± 0.05^{a}	97.42 ± 0.04^{a}	95.17 ± 0.09^{a}	75.8 ± 0.38^{f}	93.12 ± 0.10^{d}	20.11 ± 0.39^{f}	66.62 ± 0.09^{a}	93.60 ± 0.11^{a}	95.38 ± 0.11^{a}	95.86 ± 0.09^{a}	93.10 ± 0.11^{e}
12 min	92.72 ± 0.10^{b}	3.38 ± 0.11^{g}	90.07 ± 0.09^{c}	2.11 ± 0.07h	95.17 ± 0.08^{c}	1.98 ± 0.07^{g}	47.09 ± 0.30^{b}	55.17 ± 0.38^{h}	83.40 ± 0.31g	81.71 ± 0.31^{c}	59.60 ± 0.40^{c}
18 min	89.13 ± 0.11^{c}	0.08 ± 0.00^{h}	84.84 ± 0.15$^{d, e}$	0.29 ± 0.00h	96.46 ± 0.06^{g}	3.53 ± 0.12^{g}	30.27 ± 0.28^{c}	57.86 ± 0.38^{g}	68.23 ± 0.39^{f}	58.90 ± 0.38g	51.61 ± 0.42^{d}
24 min	87.57 ± 0.09^{d}	37.67 ± 0.56^{a}	84.35 ± 0.16^{e}	10.05 ± 0.30^{e}	95.70 ± 0.05^{b}	20.38 ± 0.41^{f}	68.10 ± 0.34g	67.71 ± 0.31^{f}	68.30 ± 0.34^{f}	68.51 ± 0.36^{f}	67.00 ± 0.37^{b}
30 min	80.67 ± 0.10g	45.82 ± 0.62^{f}	86.30 ± 0.13^{b}	31.67 ± 0.51^{d}	96.51 ± 0.05^{g}	33.01 ± 0.54^{d}	68.50 ± 0.25g	79.02 ± 0.25^{d}	73.00 ± 0.30^{d}	79.49 ± 0.28^{d}	82.00 ± 0.27^{a}
36 min	79.26 ± 0.09h	35.34 ± 0.54^{a}	88.38 ± 0.12^{f}	49.43 ± 0.60^{c}	97.25 ± 0.02^{e}	38.83 ± 0.58^{c}	81.55 ± 0.25^{f}	73.10 ± 0.22^{e}	78.50 ± 0.26^{c}	83.70 ± 0.24^{b}	85.35 ± 0.23^{h}
42 min	74.68 ± 0.11^{j}	50.76 ± 0.63^{e}	85.41 ± 0.13^{d}	65.66 ± 0.61^{b}	96.36 ± 0.05^{g}	45.86 ± 0.63^{b}	82.85 ± 0.25$^{e, f}$	80.90 ± 0.22^{c}	81.48 ± 0.24^{b}	86.77 ± 0.22^{h}	86.40 ± 0.21$^{g, h}$
48 min	77.89 ± 0.10^{i}	59.17 ± 0.63^{d}	88.19 ± 0.12^{f}	69.68 ± 0.58^{a}	98.04 ± 0.02^{a}	53.18 ± 0.65^{a}	83.19 ± 0.24^{e}	84.88 ± 0.19^{b}	83.65 ± 0.23g	87.45 ± 0.20^{h}	87.52 ± 0.19$^{f, g}$
54 min	82.04 ± 0.09^{f}	62.06 ± 0.60^{c}	89.82 ± 0.10^{c}	73.19 ± 0.55g	96.97 ± 0.03$^{e, f}$	59.54 ± 0.64^{e}	85.64 ± 0.23^{d}	86.42 ± 0.19^{i}	85.54 ± 0.22^{e}	87.92 ± 0.21^{h}	88.01 ± 0.19^{f}
60 min	85.40 ± 0.08^{e}	76.47 ± 0.51^{b}	87.79 ± 0.10^{f}	74.04 ± 0.52$^{f, g}$	96.85 ± 0.03^{f}	62.36 ± 0.63^{e}	86.99 ± 0.22^{d}	86.33 ± 0.18^{i}	84.29 ± 0.23$^{e, g}$	76.83 ± 0.19^{e}	92.64 ± 0.12^{e}
*a**											
6 min	− 0.31 ± 0.11^{a}	− 0.27 ± 0.10^{d}	− 0.13 ± 0.19^{a}	5.78 ± 0.78^{e}	− 0.23 ± 0.20^{a}	20.71 ± 0.13^{e}	0.27 ± 0.20^{b}	− 0.03 ± 0.22^{a}	− 0.02 ± 0.25^{a}	− 0.09 ± 0.21^{d}	0.01 ± 0.24^{c}
12 min	− 0.39 ± 0.20^{a}	6.23 ± 0.07^{b}	0.74 ± 0.32^{a}	7.05 ± 0.31^{e}	− 0.36 ± 0.16^{a}	8.31 ± 0.47^{b}	3.22 ± 0.62$^{a, c}$	6.70 ± 0.69^{b}	2.12 ± 0.67$^{a, d}$	1.93 ± 0.66$^{c, d}$	1.58 ± 0.13$^{c, d}$
18 min	0.09 ± 0.20$^{a, b}$	0.22 ± 0.02^{d}	0.84 ± 0.31^{a}	1.14 ± 0.08^{a}	− 0.48 ± 0.12^{a}	18.37 ± 1.29^{e}	5.82 ± 0.47^{a}	7.32 ± 0.64^{b}	5.94 ± 0.74^{b}	6.32 ± 0.69^{a}	6.30 ± 0.74^{b}
24 min	0.06 ± 0.17$^{a, b}$	28.72 ± 0.32^{e}	0.53 ± 0.26^{a}	24.41 ± 0.48$^{b, c}$	− 0.18 ± 0.10^{a}	35.89 ± 0.76^{d}	4.96 ± 0.64$^{a, c}$	5.10 ± 0.51$^{b, c}$	5.07 ± 0.62$^{b, c}$	4.99 ± 0.68$^{a, b}$	9.06 ± 0.73^{a}
30 min	0.79 ± 0.19$^{b, c}$	28.34 ± 0.53^{e}	0.56 ± 0.23^{a}	27.82 ± 0.16^{b}	− 0.19 ± 0.09^{a}	36.56 ± 0.22^{d}	2.84 ± 0.47$^{b, c}$	3.97 ± 0.40^{c}	4.61 ± 0.51$^{b, c, d}$	2.90 ± 0.55$^{b, c}$	6.05 ± 0.69^{b}
36 min	0.89 ± 0.18$^{b, c}$	29.01 ± 0.22^{e}	0.81 ± 0.26^{a}	23.25 ± 0.72^{c}	− 0.32 ± 0.05^{a}	33.58 ± 0.12$^{c, d}$	2.80 ± 0.46$^{b, c}$	3.82 ± 0.32^{c}	3.81 ± 0.43$^{b, c, d}$	2.14 ± 0.46$^{c, d}$	3.39 ± 0.49^{d}
42 min	1.32 ± 0.19^{c}	27.27 ± 0.61^{e}	0.7 ± 0.22^{a}	17.86 ± 0.99^{d}	− 0.07 ± 0.09^{a}	31.00 ± 0.39^{c}	2.86 ± 0.44$^{b, c}$	4.04 ± 0.26^{c}	3.58 ± 0.37$^{b, c, d}$	2.01 ± 0.40$^{c, d}$	2.72 ± 0.39^{d}
48 min	1.18 ± 0.19^{c}	21.91 ± 0.83^{c}	0.48 ± 0.20^{a}	14.81 ± 1.00$^{d, f}$	− 0.17 ± 0.05^{a}	26.62 ± 0.69^{a}	2.70 ± 0.42$^{b, c}$	3.60 ± 0.19^{c}	3.19 ± 0.33$^{c, d}$	1.86 ± 0.38$^{c, d}$	2.88 ± 0.32^{d}
54 min	1.07 ± 0.16^{c}	20.41 ± 0.83^{c}	0.82 ± 0.21^{a}	13.26 ± 0.94^{f}	0.04 ± 0.06^{a}	21.98 ± 0.87^{e}	2.59 ± 0.40$^{b, c}$	3.94 ± 0.13^{c}	3.13 ± 0.30$^{c, d}$	1.98 ± 0.38$^{c, d}$	2.83 ± 0.24^{d}
60 min	0.76 ± 0.15$^{b, c}$	10.16 ± 1.00^{a}	0.52 ± 0.17^{a}	12.21 ± 0.90^{f}	− 0.05 ± 0.06^{a}	18.54 ± 0.98^{e}	2.47 ± 0.38$^{b, c}$	4.21 ± 0.08^{c}	3.54 ± 0.29$^{b, c, d}$	1.71 ± 0.35$^{c, d}$	3.11 ± 0.20^{d}
*b**											
6 min	3.92 ± 0.03^{c}	3.39 ± 0.03^{d}	6.33 ± 0.02^{g}	27.15 ± 0.13^{e}	7.25 ± 0.04^{a}	31.72 ± 0.49^{b}	6.69 ± 0.01^{j}	7.58 ± 0.02^{h}	7.68 ± 0.01^{j}	7.01 ± 0.02^{j}	8.25 ± 0.03^{i}
12 min	8.07 ± 0.08^{d}	5.22 ± 0.16^{c}	10.86 ± 0.00^{i}	3.40 ± 0.12^{g}	6.20 ± 0.06^{b}	3.15 ± 0.11^{d}	22.70 ± 0.02^{b}	29.26 ± 0.04^{a}	23.17 ± 0.02^{c}	23.41 ± 0.05^{c}	30.32 ± 0.02^{b}
18 min	8.02 ± 0.06^{d}	− 0.07 ± 0.00^{e}	10.87 ± 0.00^{i}	0.28 ± 0.01^{h}	4.61 ± 0.05^{c}	5.70 ± 0.21^{c}	21.56 ± 0.04^{c}	28.34 ± 0.06^{b}	29.74 ± 0.02^{a}	28.92 ± 0.03^{a}	33.26 ± 0.05^{a}
24 min	6.64 ± 0.04^{g}	53.62 ± 0.34^{g}	9.19 ± 0.01^{a}	16.88 ± 0.49^{f}	3.93 ± 0.03^{d}	34.36 ± 0.67^{a}	25.74 ± 0.03^{a}	22.01 ± 0.04^{c}	25.23 ± 0.03^{b}	26.72 ± 0.02^{b}	28.07 ± 0.04^{c}
30 min	7.15 ± 0.00^{e}	55.59 ± 0.31^{f}	8.23 ± 0.01^{c}	47.75 ± 0.47^{i}	3.38 ± 0.02^{e}	53.11 ± 0.67^{f}	18.09 ± 0.01^{d}	18.08 ± 0.02^{d}	21.74 ± 0.03^{d}	20.60 ± 0.01^{d}	19.64 ± 0.00^{d}
36 min	6.65 ± 0.01^{g}	51.01 ± 0.42^{h}	8.92 ± 0.01^{b}	51.65 ± 0.25^{a}	2.14 ± 0.03$^{f, g}$	57.44 ± 0.43^{e}	17.80 ± 0.00^{e}	16.00 ± 0.00^{i}	18.92 ± 0.01^{e}	17.17 ± 0.01^{e}	16.38 ± 0.02^{e}
42 min	7.13 ± 0.03$^{e, f}$	54.43 ± 0.35$^{f, g}$	7.67 ± 0.00^{d}	48.43 ± 0.25^{i}	3.32 ± 0.02^{e}	58.28 ± 0.27^{e}	17.38 ± 0.01^{f}	15.75 ± 0.02^{i}	17.35 ± 0.01^{f}	15.28 ± 0.01^{f}	14.90 ± 0.01^{f}
48 min	6.94 ± 0.03^{f}	49.70 ± 0.34^{h}	6.91 ± 0.00^{f}	44.46 ± 0.22^{b}	1.98 ± 0.02^{g}	57.14 ± 0.25^{e}	17.21 ± 0.01^{g}	14.10 ± 0.06^{e}	16.03 ± 0.02^{h}	14.47 ± 0.02^{h}	13.68 ± 0.04^{g}
54 min	5.83 ± 0.03^{a}	47.54 ± 0.32^{a}	7.17 ± 0.02^{e}	41.44 ± 0.19^{c}	2.28 ± 0.00^{f}	54.14 ± 0.21^{f}	16.51 ± 0.01^{h}	13.77 ± 0.07^{f}	15.67 ± 0.03^{i}	14.72 ± 0.01^{g}	13.08 ± 0.04^{h}
60 min	5.11 ± 0.02^{b}	36.10 ± 0.25^{b}	5.84 ± 0.01^{h}	39.25 ± 0.17^{d}	2.14 ± 0.01$^{f, g}$	52.88 ± 0.15^{f}	15.76 ± 0.01^{i}	13.26 ± 0.07^{g}	16.39 ± 0.04^{g}	12.85 ± 0.00^{i}	8.09 ± 0.03^{i}
h°											
6 min	85.47 ± 1.63$^{a, b}$	85.52 ± 1.63^{a}	88.28 ± 1.18^{a}	77.98 ± 1.63^{e}	88.21 ± 1.55^{a}	56.86 ± 0.56$^{h, i}$	87.73 ± 1.67^{a}	88.34 ± 0.23^{a}	88.17 ± 0.11^{a}	88.28 ± 0.74^{a}	88.33 ± 0.06^{a}
12 min	87.22 ± 1.44$^{a, b}$	39.94 ± 0.50^{c}	86.13 ± 1.65^{a}	25.74 ± 0.21^{c}	86.71 ± 1.46^{a}	20.78 ± 0.41^{b}	81.93 ± 1.53$^{a, b}$	77.12 ± 1.31^{b}	84.79 ± 1.63$^{a, b}$	85.31 ± 1.58$^{b, c}$	87.03 ± 0.24^{a}
18 min	88.58 ± 0.63$_{a}$	17.78 ± 1.51^{d}	85.61 ± 1.60^{a}	13.83 ± 0.46^{d}	84.11 ± 1.48^{a}	17.26 ± 0.56^{c}	74.89 ± 1.19^{b}	75.52 ± 1.24^{b}	78.72 ± 1.37$^{b, c}$	77.68 ± 1.32^{b}	79.28 ± 1.25^{d}
24 min	88.58 ± 0.47^{a}	61.83 ± 0.41$^{e, f}$	86.70 ± 1.61^{a}	34.66 ± 0.25^{b}	87.44 ± 1.41^{a}	43.75 ± 0.05^{a}	79.11 ± 1.39^{b}	76.97 ± 1.30^{b}	78.64 ± 1.37$^{b, c}$	79.44 ± 1.40^{b}	72.13 ± 1.36$^{b, c}$
30 min	83.74 ± 1.46$^{a, b}$	62.99 ± 0.56$^{e, f}$	86.11 ± 1.59^{a}	59.77 ± 0.39^{a}	86.77 ± 1.55^{a}	55.46 ± 0.18^{i}	81.10 ± 1.44$^{a, b}$	77.62 ± 1.22^{b}	78.04 ± 1.31^{c}	81.99 ± 1.50$^{b, c}$	72.91 ± 1.82$^{b, c, d}$
36 min	82.42 ± 1.49$^{a, b}$	60.38 ± 0.39^{e}	84.85 ± 1.63^{a}	65.77 ± 0.76^{f}	81.61 ± 1.29^{a}	59.69 ± 0.28$^{g, h}$	81.08 ± 1.43$^{a, b}$	76.57 ± 1.09^{b}	78.63 ± 1.24$^{b, c}$	82.90 ± 1.51$^{b, c}$	78.33 ± 1.62$^{c, d}$
42 min	79.55 ± 1.48^{b}	63.39 ± 0.66$^{e, f}$	84.79 ± 1.63^{a}	69.76 ± 1.13$^{f, g}$	88.44 ± 1.22^{a}	61.99 ± 0.41$^{f, g}$	80.68 ± 1.43$^{a, b}$	75.61 ± 0.87^{b}	78.34 ± 1.17$^{b, c}$	82.53 ± 1.45$^{b, c}$	79.66 ± 1.44^{d}

Table 3 (continued)

Parameters	T1	T2	T3	T4	T5	T6	T7	T8	T9	T10	T11
48 min	80.38 ± 1.53^{b}	66.21 ± 0.95^{f}	86.03 ± 1.65^{a}	71.58 ± 1.24^{g}	85.07 ± 1.48^{a}	$65.02 \pm 0.66^{e,f}$	$81.11 \pm 1.38^{a,b}$	75.70 ± 0.65^{b}	$78.77 \pm 1.10^{b,c}$	$82.70 \pm 1.45^{b,c}$	$78.12 \pm 1.25^{c,d}$
54 min	79.65 ± 1.53^{b}	66.77 ± 0.99^{f}	83.48 ± 1.67^{a}	72.27 ± 1.26^{g}	88.49 ± 1.00^{a}	$67.91 \pm 0.87^{d,e}$	$81.09 \pm 1.35^{a,b}$	74.03 ± 0.43^{b}	$78.71 \pm 1.03^{b,c}$	$82.36 \pm 1.43^{b,c}$	$77.80 \pm 0.97^{c,d}$
60 min	$81.60 \pm 1.62^{a,b}$	74.28 ± 1.58^{b}	84.91 ± 1.67^{a}	$72.72 \pm 1.27^{e,g}$	88.39 ± 1.34^{a}	70.69 ± 1.00^{d}	$81.11 \pm 1.32^{a,b}$	72.41 ± 0.21^{b}	77.82 ± 0.94^{c}	$82.45 \pm 1.51^{b,c}$	68.97 ± 1.15^{b}

phenolic compounds associated with reddish and yellowish colors (Ali et al., 2019).

For the extracts and hydrolysates obtained in the hydrothermal process, the $h°$ angles varied between 17.26 and 88.58. Regarding extraction temperatures, the extracts have hue angles exceeding 79.55°, suggesting a tendency towards yellow color. In contrast, hydrolyzed at 100 °C, display hue angles range from 68.97 to 88.34, indicating a color between red and yellow. For hydrolysates at temperatures of 143 °C and 160 °C, the $h°$ values indicate a brown coloration, aligning with the coloration seen in Fig. 2.

pH

According to the kinetic curves of the pH (Fig. 3), it is possible to establish that throughout the process of extraction and hydrolysis of 11 tests, pH tended to increase, a trend that was also reported by Castro et al. (2023) for grape pomace. However, within the first 6 min of extraction, a decrease in pH is evident, attributed to the consumption of amino groups and the release of organic acids in the initial stage of the process (Li et al., 2021). Its subsequent increase is associated with the neutralization of organic acids and the formation of products from Maillard reactions (Ferreira et al., 2023). In addition, it was observed that the pH was influenced by temperature, presenting a variation between 2.98 (T1) and 7.87 (T6). Extraction tests (T1, T3, and T5) presented the lowest pH results during the 60 min of the process, reaching a maximum pH value of 4.1. On the other hand, hydrolysis temperatures favored the increase in the pH of the obtained hydrolysates (T6). Similar results were obtained for jabuticaba peel extracts/hydrolysates (Barroso et al., 2022a, b), soybean residues (Vedovatto et al., 2021), and brewers' spent grains (Sganzerla et al., 2022). This behavior could be related to the decrease in amino acids because of the interaction between amino groups with reducing sugars during the Maillard reaction (Jeong et al., 2021), to the neutralization of organic acids (Ferreira et al., 2023), and an increase of [OH−] ions by self-ionization due to high temperatures and pressure (Ahmed & Chun, 2018; Park et al., 2015).

Antioxidant Activity

Figure 4 illustrates the antioxidant capacity of the cambuci peel extracts/hydrolysates as assessed using the DPPH and FRAP tests. The DPPH method revealed that the antioxidant capacity of tests conducted at 100 °C exhibited a linear trend from 6 to 60 min, with values ranging between 5.60 and 6.21 μmol TEAC g^{-1}. Moreover, hydrolysates obtained at higher temperatures (T2, T4, and T6) yielded lower antioxidant capacity values, ranging from 3.18 to 6.11 μmol TEAC g^{-1}. An explanation for this could be the degradation of tannins because of high temperatures (Pinto et al., 2021).

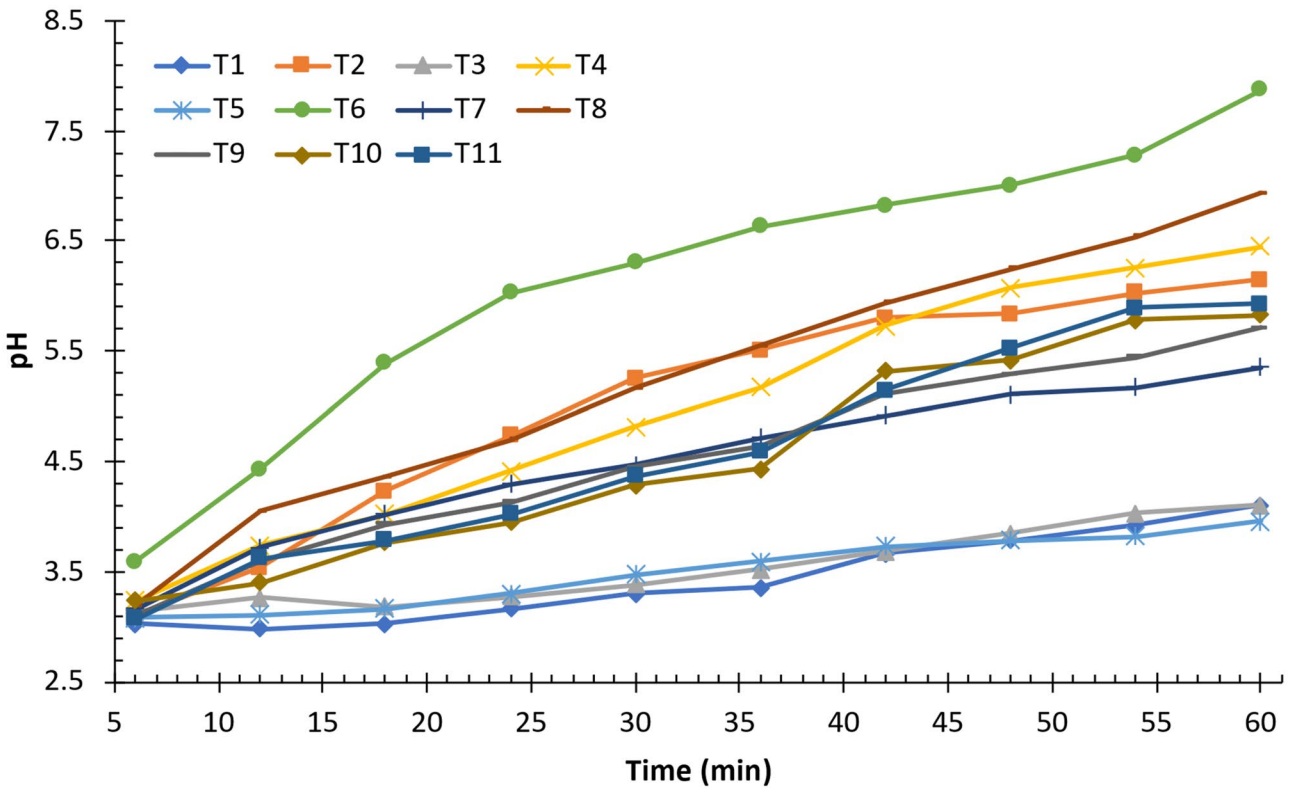

Fig. 3 pH of the samples extracted from the cambuci peel using hydrothermal processing

For the T1 and T3 extraction tests, carried out at 57 °C, a decrease in antioxidant capacity was obtained after 36 and 42 min of extraction, respectively. The test carried out at 40 °C presented a marked decrease after 24 min of the process. Similar results were obtained by Bodoira et al. (2019) for Pistachio (*Pistacia vera* L.) nuts extract. The accumulated values of antioxidant capacity by the DPPH method (Fig. 4b) allowed to establish that T7 (100 °C and pH 4) had a greater antioxidant capacity (61.41 µmol TEAC g^{-1}).

The FRAP assay revealed that high temperatures favor antioxidant capacity (Fig. 4c). The maximum value of all the kinetics was obtained at 160 °C and pH 5.5 (118.07 µmol TEAC g^{-1}), followed by 107.28 µmol TEAC g^{-1} and 45.26 µmol TEAC g^{-1} (T2 and T4, respectively), obtained at the 18 min of the process. Similar behavior was observed by Gan and Baroutian (2022) from New Zealand Wakame (*Undaria pinnatifida*) seaweed. Furthermore, the results of antioxidant capacity by this method show a behavior similar to that of phenolic compounds, which indicates a possible correlation between these parameters. Also, it was evident that the extraction temperatures of 40 and 57 °C exhibited the lowest levels of antioxidant capacity throughout the 60-min extraction period, the values oscillated between 4.24 and 19.34 µmol TEAC g^{-1} for T1, between 4.84 and 11.83 µmol TEAC g^{-1} for T3, and between 3.06 and 11.37 µmol TEAC g^{-1} for T5. The cumulative values of antioxidant capacity for this assay (Fig. 4d) revealed that the most favorable condition for antioxidant capacity was T6 (160 °C and pH 5.5), and the most unfavorable condition was T5 (40 °C and pH 5.5).

The antioxidant capacity for the DPPH and FRAP assays was assessed using a central composite rotational design (CCRD) with two independent variables: temperature and pH (Table 1). In the DPPH method, the significant coefficients were associated with temperature (both linear and quadratic terms) and pH (linear term). This method yielded a coefficient of determination (R^2) value of 0.9581. For the FRAP method, the significant coefficients were linear and quadratic temperature, presenting an R^2 of 0.9797, which suggests that the models effectively match the selected parameters. The models for the DPPH and FRAP assays are shown below:

$$\begin{aligned}\text{DPPH} &= 53.5924 + 0.3118 \cdot (\text{Temperature}) \\ &\quad - 0.0018 \cdot (\text{Temperature}^2) \\ &\quad - 1.384 \cdot (\text{pH}), (R^2 \ \text{Adj} = 0.9162)\end{aligned}$$

$$\begin{aligned}\text{FRAP} &= 169.8880 - 3.6345 \cdot (\text{Temperature}) \\ &\quad + 0.0356 \cdot (\text{Temperature}^2), (R^2 \ \text{Adj} = 0.9593)\end{aligned}$$

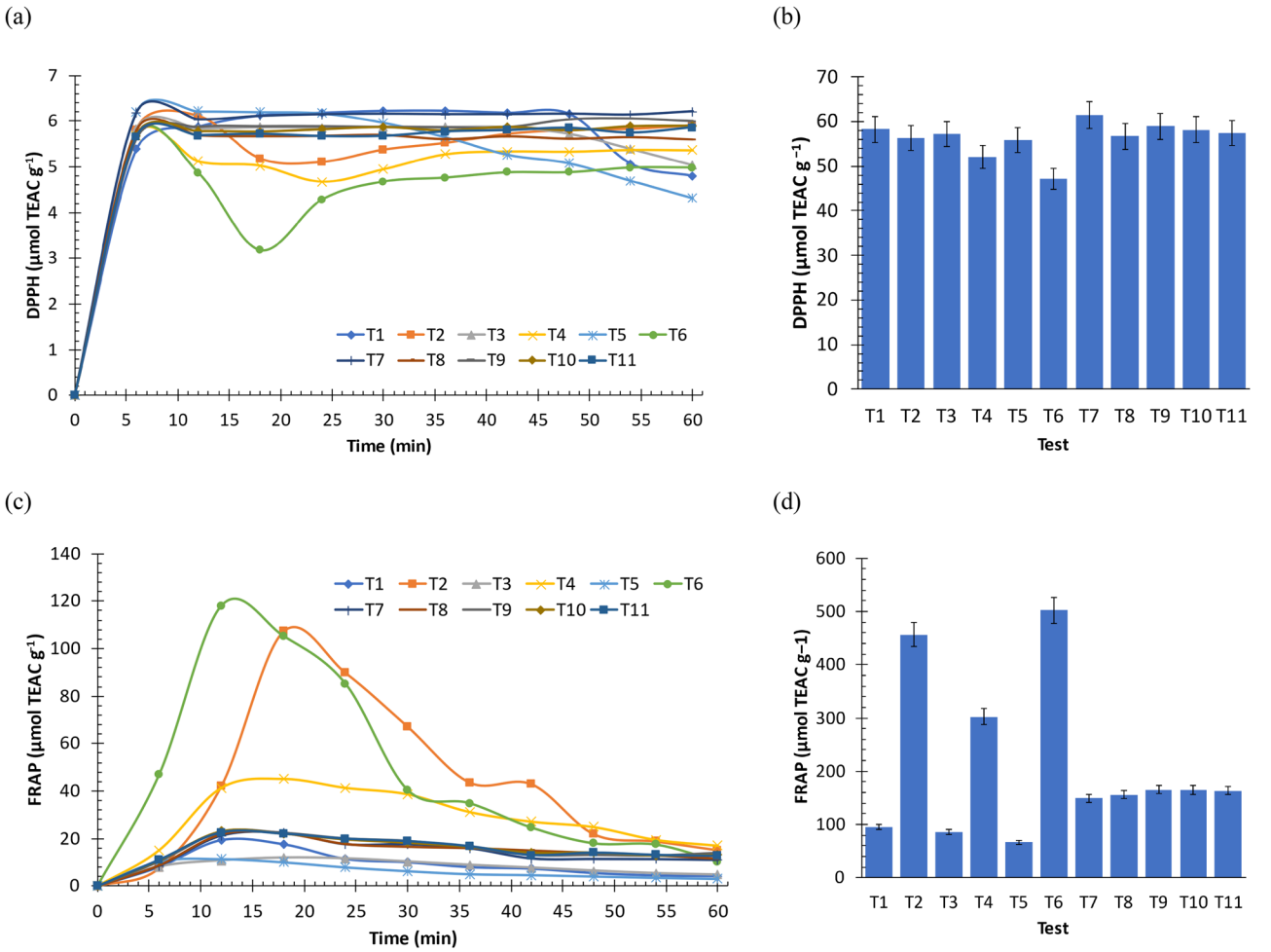

Fig. 4 Antioxidant activity of the samples extracted from the cambuci peel using hydrothermal processing. **a** DPPH; **b** accumulated DPPH; **c** FRAP; **d** accumulated FRAP

The optimization results for the antioxidant capacity by the DPPH assay were Temp = 79.6 °C, pH = 6.4, and DPPH = 58.15 µmol TEAC g^{-1}. For the FRAP essay, the optimization parameters were Temp = 160 °C and FRAP = 500.24 µmol TEAC g^{-1}. By performing the hydrolysis again at 160 °C, it was possible to determine that the antioxidant capacity accumulated by the FRAP method was 483.72 µmol of TEAC g^{-1}, which differs by 3.3% from the value predicted by the model obtained. The behavior of the antioxidant capacity as determined by the FRAP test closely resembled the results reported by Ferreira et al. (2023), who studied the extracts and hydrolysates of pitaya residues using a high-pressure hydrothermal process. However, for the antioxidant activity by the DPPH assay, there was a variation in behavior, which could be attributed to the fact that DPPH has a reduced solubility in aqueous media, which means that this radical has a low availability to interact with antioxidant compounds (Angonese et al., 2021). Furthermore, the pigmentation of some compounds present in the samples could also interfere with absorption due to the spectra overlapping (Yeo & Shahidi, 2019).

Figure 5 illustrates the behavior of antioxidant capacity (DPPH, FRAP, and TPC). Noticeably, the lowest values correspond to the green areas, while the highest values are found in the red or brown areas. This provides an insight into the range of values that these variables can assume for different combinations of temperature and pH. In the case of DPPH, it is evident that both pH and temperature impact the analyzed response (Fig. 5a, b). This suggests that at temperatures around 80 °C and low pH, better antioxidant capacity yields could be generated when employing this method. On the other hand, regarding the FRAP method, it can be concluded that pH does not affect the response variable; instead, it is solely influenced by the temperature of the process.

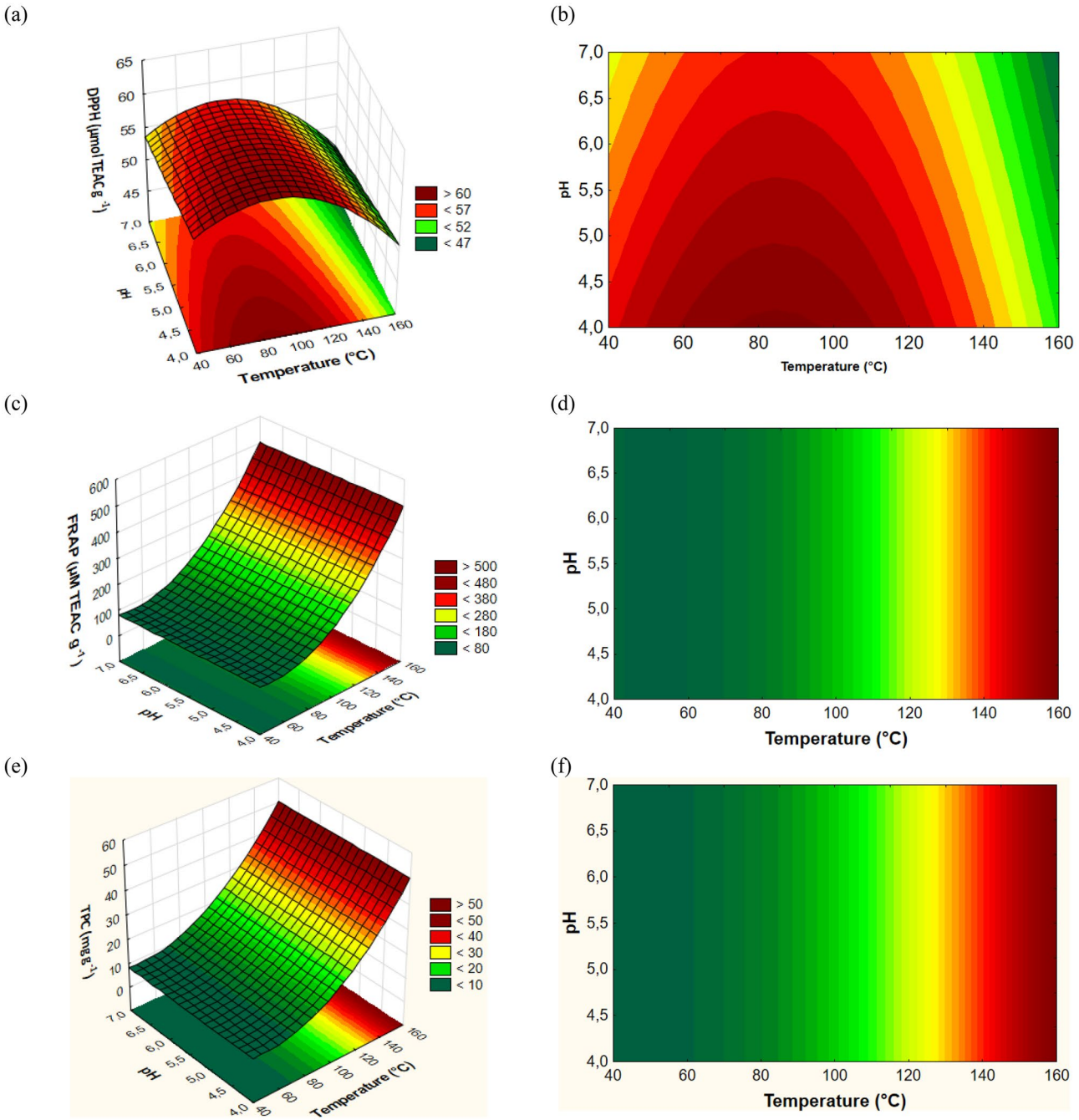

Fig. 5 The influence of temperature and pH on the antioxidant capacity of cambuci peel hydrolysates. **a** DPPH response surface; **b** DPPH contour curve; **c** FRAP response surface; **d** FRAP contour curve; **e** TPC response surface; **f** TPC contour curve

Total Phenolic Compounds

Phenolic compounds were monitored in extracts and hydrolysates of cambuci peel, and the results are presented in Fig. 6. It was observed that the greatest concentration of phenolic compounds was obtained mainly between 12 and 18 min of extraction/hydrolysis. Likewise, it was possible to establish that the hydrolysates at 143 and 160 °C (T2, T4, and T6) presented a higher concentration of phenolic compounds, with maximum values of 12.44 mg g^{-1} (T2), 9.50 mg GAE g^{-1} (T4), and 12.76 mg GAE g^{-1} (T6). Moreover, it was established that extraction temperatures (40 and 57 °C) did not favor the concentration of TPC in the extracts since these tests obtained the lowest concentrations, varying between 0.35 and 1.97 mg GAE g^{-1}. The accumulated concentration of the extracts and hydrolysates of the cambuci

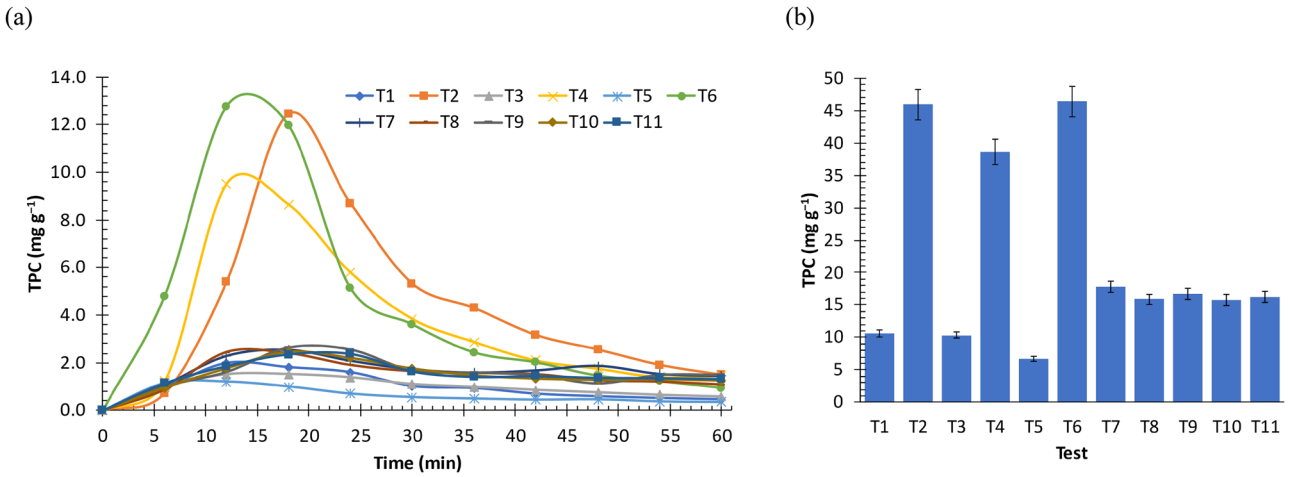

Fig. 6 Kinetic and accumulated performance of total phenolic compounds (TPC) from the cambuci peel through hydrothermal processing. **a** TPC; **b** accumulated TPC

peel presented in Fig. 6b makes it easier to visualize the behavior described above. The maximum accumulated concentration of TPC was obtained at 160 °C (46.40 mg GAE g^{-1}), and the lowest accumulated concentration was at 40 °C (6.72 mg GAE g^{-1}).

TPC was also evaluated with a CCRD, with temperature and pH as independent variables (Fig. 5e, f). For TPC, the significant coefficients were linear and quadratic temperature, with an $R^2 = 0.9776$, thus indicating a high correlation between the data and the model presented below.

$$\text{TPC} = 15.3136 - 0.3057 \cdot (\text{Temperature}) + 0.0033 \cdot (\text{Temperature}^2), (R^2 \text{ Adj} = 0.9553)$$

For TPC, the optimization parameters were Temp = 160 °C and TPC = 50.88 mg g^{-1}. After performing the hydrolysis again at 160 °C, it was determined that the accumulated TPC was 48.3 mg g^{-1}, which differs by 5.1% from the value predicted by the model obtained. The rise in temperature and the total phenolic compound concentration can be explained by the fact that increased temperature reduces the surface tension of water. This reduction allows water to penetrate the solid matrix more easily and promotes the dilution of the compounds (Herbst et al., 2021). Results with this trend were obtained for potato peel (Singh & Saldaña, 2011), carrot leaves (Song et al., 2018), acerola pomace (Mesquita et al., 2022), and pitaya peel (Ferreira et al., 2023).

Reducing Sugars

The kinetic profile of reducing sugars is presented in Fig. 7. For the tests, the highest yield was obtained during

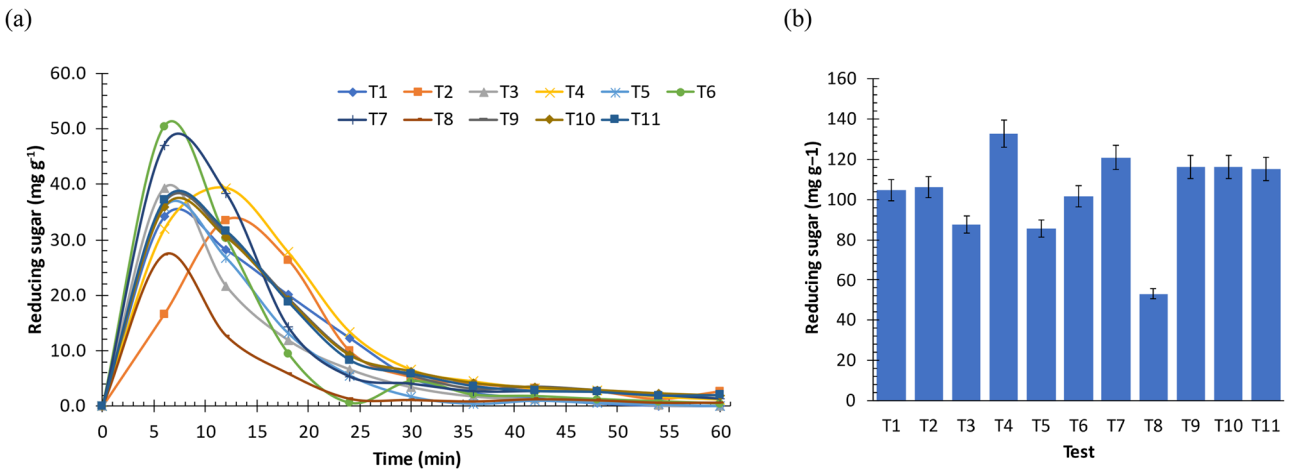

Fig. 7 Kinetic and accumulated performance of the production of reducing sugars obtained from the cambuci peel hydrothermal processing. **a** Reducing sugars; **b** accumulated reducing sugars

the first 12 min of the extraction/hydrolysis process. In all cases, the kinetics decrease after reaching the highest yield, achieving stabilization after 30 min. The extraction tests presented a maximum reducing sugar yield between 34.20 and 39.35 mg g^{-1}. Meanwhile, the hydrolysis tests carried out at temperatures of 100 and 160 °C presented the highest yields of reducing sugars between 27.33 and 50.42 mg g^{-1}. In the case of the tests carried out at 143 °C (T2 and T4), the reducing sugars obtained were 33.56 and 39.33 mg g^{-1}, respectively. After the first 6 min of extraction/hydrolysis, T6 (160 °C and pH 5.5) was the test with the highest yield of reducing sugars, which could be attributed to an increase in the ionization constant of water at high temperature and pressure (Ahmed & Chun, 2018; Park et al., 2015). These results favor the increase of H^+ and OH^- ions and facilitate the hydrolysis of cellulose and hemicellulose to monosaccharides (Pattnaik et al., 2021).

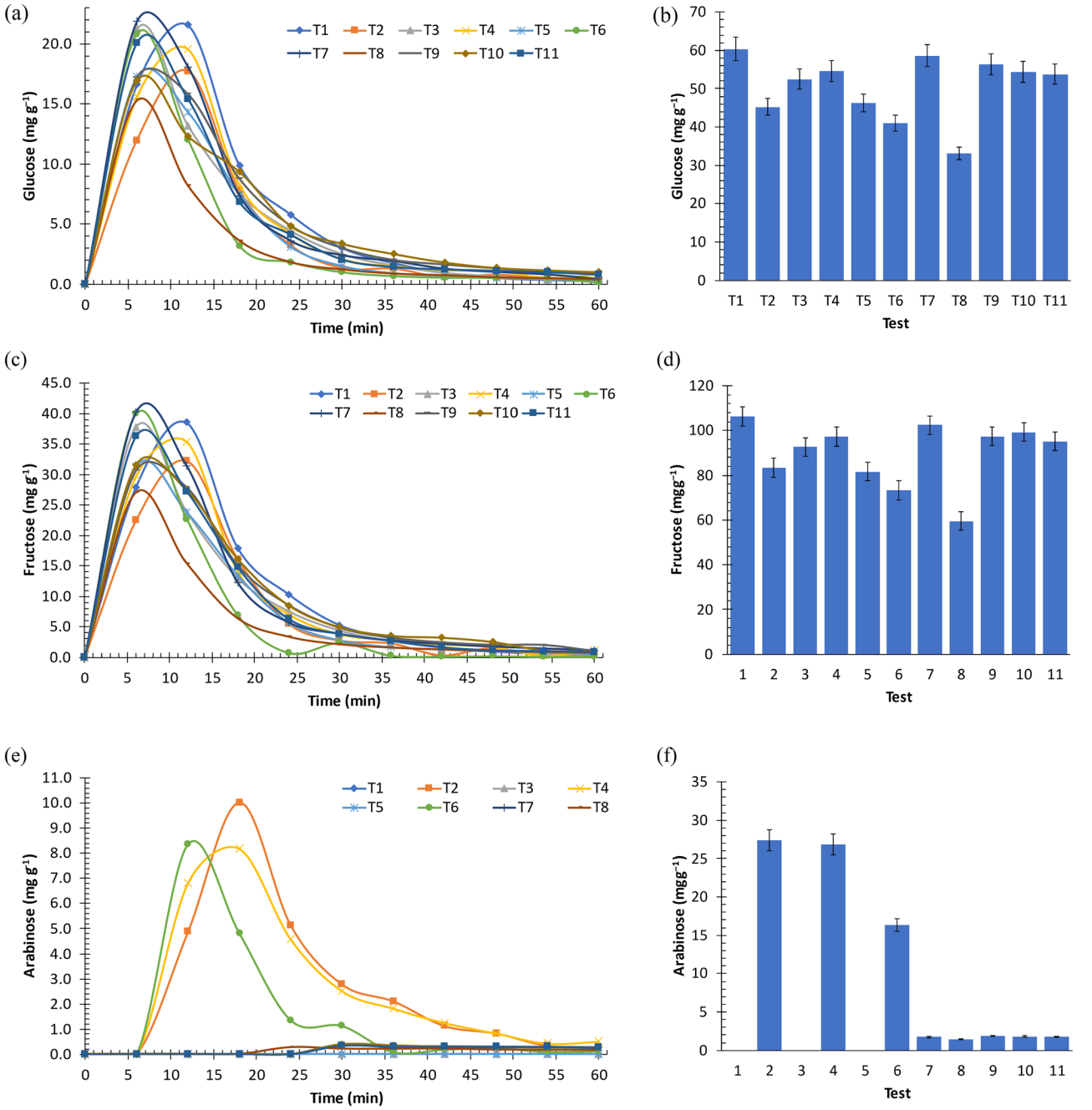

Fig. 8 Kinetic and accumulated performance of monosaccharides obtained from the cambuci peel through hydrothermal processing. **a** Glucose; **b** accumulated glucose; **c** fructose; **d** accumulated fructose; **e** arabinose; **f** accumulated arabinose

From the kinetics of reducing sugars, it is possible to determine that until 30 min (process stabilization), a higher recovery of 86.69% (m/m) is achieved for all extraction and hydrolysis tests. This indicates that the extraction and hydrolysis process could be limited to 30 min. The accumulated values of reducing sugars at the end of the 60 min of extraction/hydrolysis are presented in Fig. 7b. T4 obtained the highest accumulated production of reducing sugars (132.54 mg g^{-1}), followed by treatment T7 with 120.75 mg g^{-1}.

Sugars, Citric Acid, and Inhibitors

The kinetics and accumulation of sugars such as glucose, fructose, and arabinose obtained in the extraction/hydrolysis process are presented in Fig. 8. The analysis revealed that the sugars that presented the best yields in the cambuci peel were glucose and fructose. The highest glucose and fructose results were obtained in T7 with 21.85 mg g^{-1} and 40.20 mg g^{-1}, respectively, 6 min after starting the process. Furthermore, it is possible to establish that between 6 and 12 min of the extraction/hydrolysis process, there are increased yields of these two monosaccharides for all the tests in the study. At the end of the extraction/hydrolysis, the treatments that obtained the highest accumulated glucose yields were T1 (57 °C and pH 4.4) (106.35 mg g^{-1}) and T7 (100 °C and pH 4.0) (102.4 mg g^{-1}), values higher than those reported for peach palm by-products (glucose 65.5 mg g^{-1}—fructose 53.5 mg g^{-1}) (Giombelli et al., 2020) and orange peel (glucose 50.8 mg g^{-1}—fructose 34.2 mg g^{-1}) (Lachos-Perez et al., 2020).

Arabinose was only present in hydrolysis tests. In the case of the tests carried out at 100 °C, the maximum yield of this monosaccharide was evident 30 min into the process. In comparison, the hydrolysates at 143 °C and 160 °C presented better yields at 18 and 12 min, respectively. The accumulated arabinose maximums were obtained in T2 (27.40 mg g^{-1}) and T4 (26.86 mg g^{-1}). The observation indicates that the monosaccharide is formed due to the hydrolysis process of polysaccharides since elevated temperatures facilitate the breakdown of lignocellulosic structures (Barroso et al., 2022a, b; Castro et al., 2023). The citric acid obtained in the extracts and hydrolysates of the cambuci peel presented its maximum values between 6 and 12 min of the process (Fig. 9), being T2 (23.50 mg g^{-1}), T4 (24.58 mg g^{-1}), and T6 (23.03 mg g^{-1}), the tests with better yields.

The 5-hydroxymethylfurfural (5-HMF) is a fermentation inhibitor that is related to the breakdown of glucose (T. C. G. Oliveira et al., 2020) and the increase in temperature (Martins-Vieira et al., 2023). This was confirmed as the inhibitor 5-HMF was only detected in hydrolysates T4 (143 °C and pH 6.6) and T6 (160 °C and pH 5.5), with accumulated concentrations of 0.87 mg g^{-1} and 0.59 mg g^{-1}, respectively. In both tests, the inhibitor was identified after 12 min of extraction. The presence of this compound in cambuci peel hydrolysates is due to the breakdown of biomass, which utilizes carbohydrates like fructose, glucose, hemicellulose, and cellulose in the formation of 5-HMF (Özkaynak Kanmaz, 2018; Pińkowska et al., 2020) (Fig. 10).

UPLC-PDA-MS Analysis

The extracts were analyzed by UPLC-PDA-MS to tentatively identify potential candidates in each extract. Considering previous reports in the literature about the metabolites already identified in the cambuci fruit (Donado-Pestana et al., 2021), it was possible to point out the potential identifications related to the compounds presented in Table 4. The results indicate that ellagic acid and digalloyl-hexoside were consistently present in the cambuci peel throughout the entire extraction period of 60 min. Notably, quercetin pentoside was observed only within 6 min of the extraction process. The quantification of ellagic acid was carried out

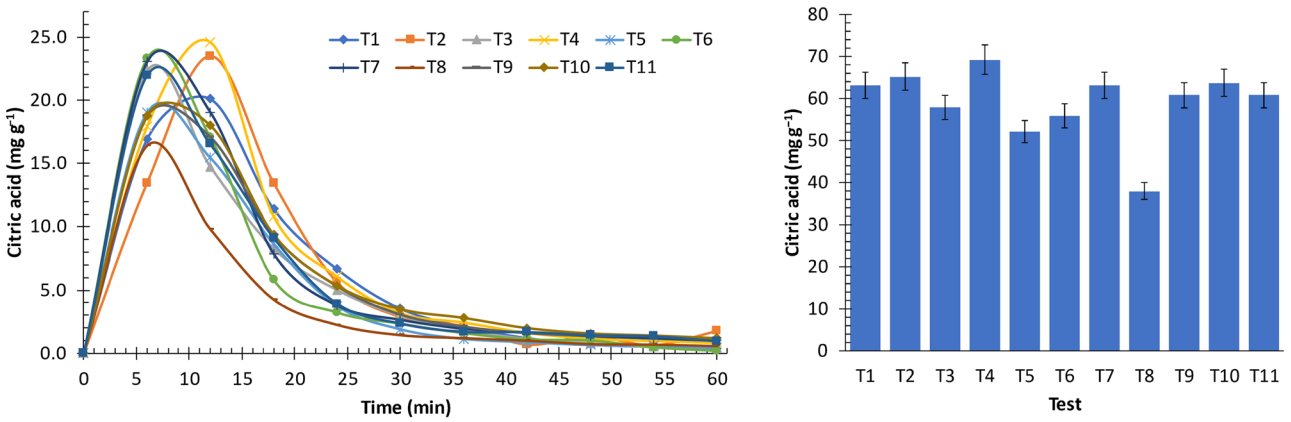

Fig. 9 Citric acid obtained from the cambuci peel through hydrothermal processing. **a** Citric acid; **b** accumulated citric acid

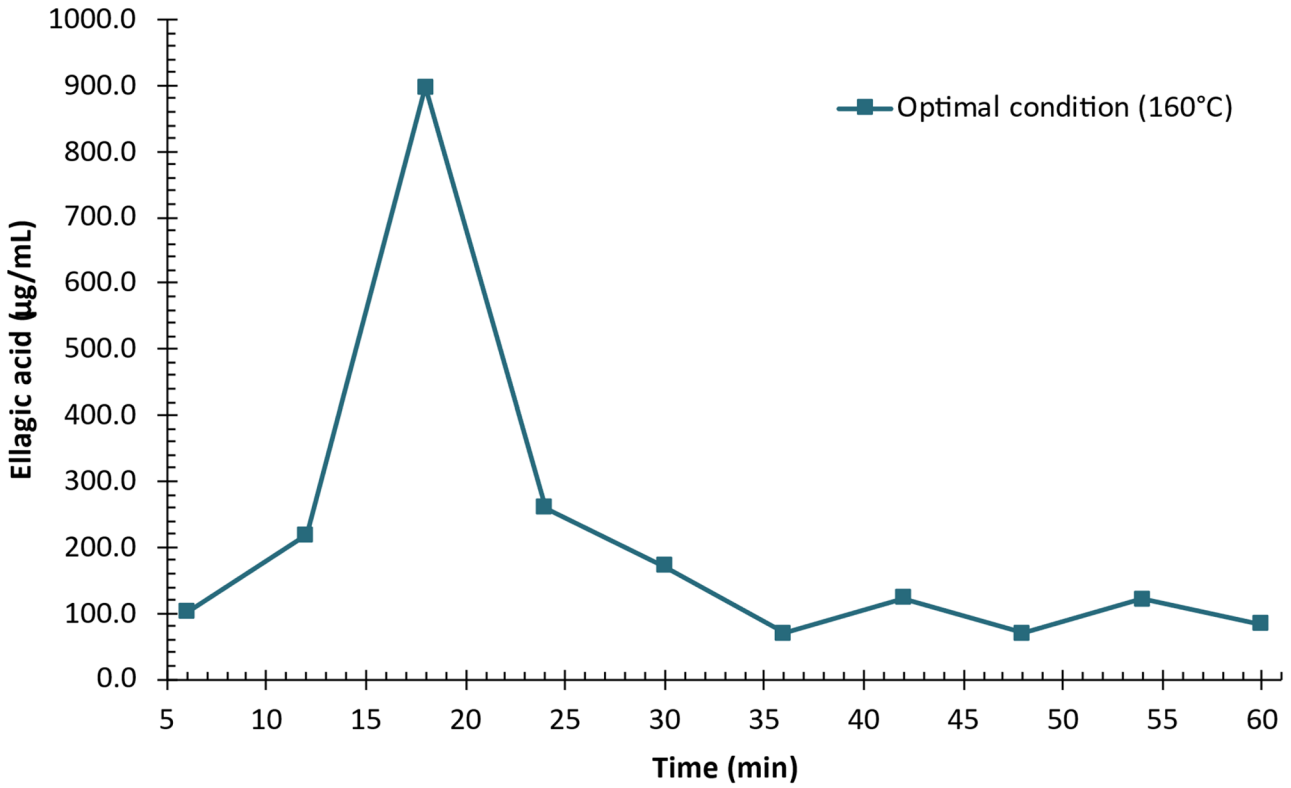

Fig. 10 Ellagic acid concentration for different extraction times in the optimal condition

due to its presence at all extraction times. Figure 10 quantifies the acid in the cambuci peel extracts in the best extraction condition (160 °C). There, it is observed that at 18 min, a higher ellagic acid content is obtained, values higher than those reported for mango pulp residue extract (200 µg/mL) (Murugan et al., 2020) and *Nigella sativa* L. straw (25.54 µg/mL) (Farouk et al., 2023).

In-line Process

The behavior of the in-line process is presented in Fig. 11. The monitoring of the process was carried out at three different wavelengths. The wavelengths were selected from the literature for compounds present in cambuci. For instance, ellagic acid was identified at 253 nm (Akter et al., 2021), galloyl-hexoside was identified at 273 nm (Aguilar-Zárate et al., 2017), and quercetin-*O*-(*O*-galloyl)-pentoside was identified at 356 nm (Saldanha et al., 2013). After 42 min, the 253 nm and 273 nm curves show near-zero absorbance, which indicates that the compounds at these wavelengths are in very low concentrations and are not easily identifiable. The 356 nm curve, starting at 36 min, begins to decrease rapidly, which indicates a decrease in the compounds identifiable at that wavelength. This information allows us to approximate when the extraction or hydrolysis process is completed in an in-line process, as the compounds of interest show a rapid decrease in concentration, sometimes reaching values that are too low for identification. For cambuci peel, this time is approximately 42 min. This method of in-line analysis enables a reduction in resource usage, minimizes the need for human intervention, and enables real-time monitoring of the entire process

Table 4 Tentative identification of metabolites present in extracts the extracts by UPLC-PDA-MS

Retention time (min)	Name	*m/z*	Lamba (λ)	Fraction	Ref.
1.1	*p*-Coumaric acid hexoside	325.17 [M-H]-	256, 291	1, 4, 5, 7, 9, 10	(Barros et al., 2012)
1.2	Digalloyl-hexoside	483.14 [M-H]-	277	1, 2, 3, 4, 5, 6, 7, 8, 9, 10	(García-Villalba et al., 2015)
3.3	Ellagic acid	301.06 [M-H]-	253, 356	1, 2, 3, 4, 5, 6, 7, 8, 9, 10	(Aguilar-Zárate et al., 2017)
3.7	Quercetin pentoside	433.22 [M-H]-	266, 364	1	(Carocho et al., 2014)

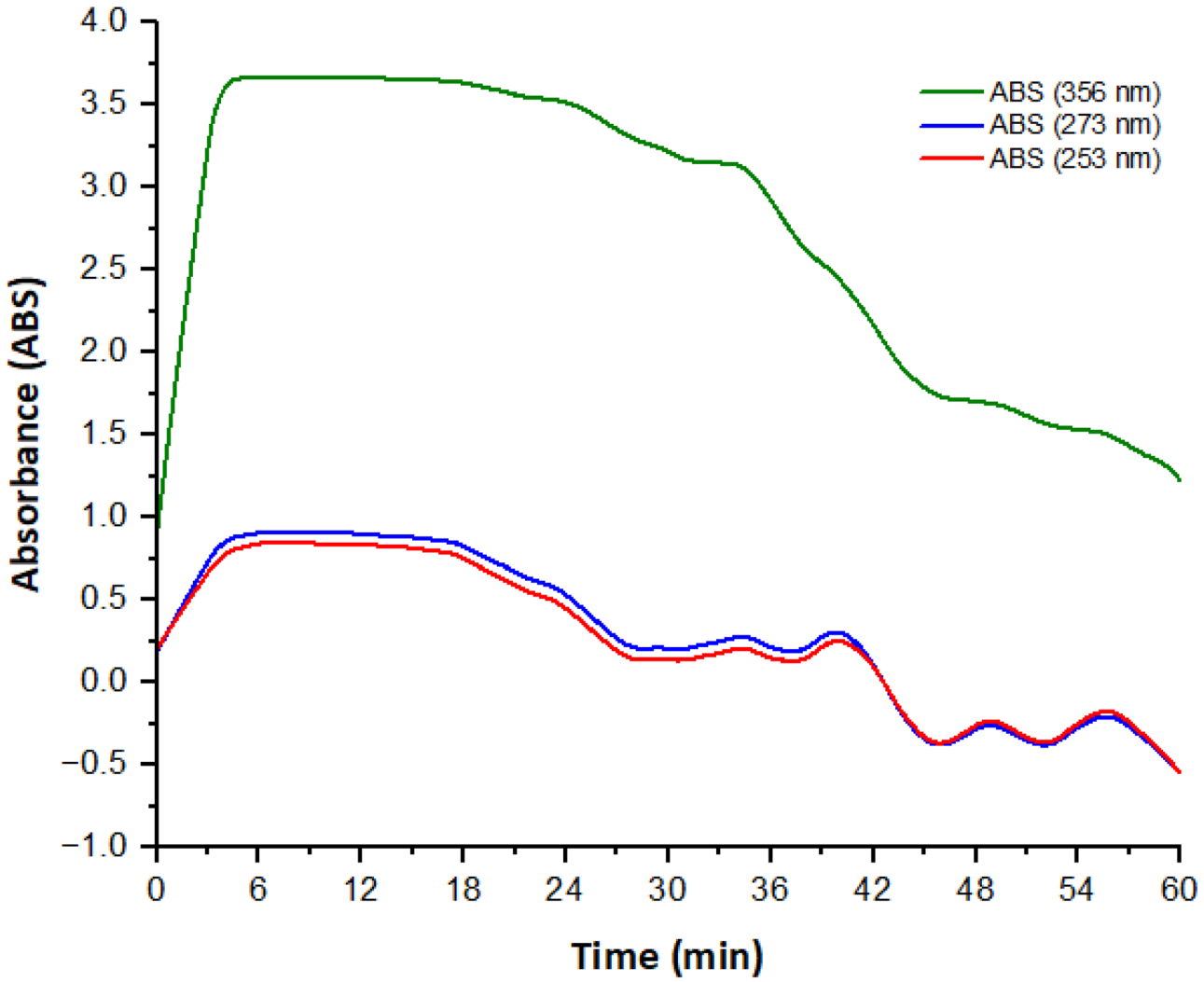

Fig. 11 In-line process monitoring at different wavelengths

(Da Silva et al., 2023). Furthermore, since the online system is automated, data collection is facilitated, which allows adequate monitoring of the process in real time (Maciel-Silva et al., 2022).

Conclusions

The hydrothermal process on semi-continuous flow is a viable alternative for the valorization of cambuci peel because it is a safe and sustainable process for the recovery of bioproducts. In the extraction and hydrolysis of the studied by-product, temperature was the predominant parameter in the analyses conducted. The antioxidant activity by the FRAP method presented a maximum yield at 160 °C (501.91 µmol of TEAC g^{-1}), as did the total phenolic compounds (46.40 mg g^{-1} of dried cambuci peel). The maximum yield of total reducing sugars (132.54 mg g^{-1}) was observed at 143 °C. Likewise, high temperatures promoted the formation of inhibitors such as 5-HMF after 12 min of the process, which is related to Maillard reaction products and fructose and glucose degradation. On the other hand, the sugars identified in the cambuci peel were glucose, arabinose, and fructose, the latter being the sugar with the highest yields (102.44 mg g^{-1}). The compounds identified in the cambuci peel were *p* - coumaric acid hexoside, digalloyl-hexoside, ellagic acid, and quercetin pentoside. The hydrothermal process was carried out for 60 min. However, in-line analysis revealed that 42 min is sufficient to recover more than 80% of the bioactive compounds. This finding suggests potential savings in time and money, which may spark industry interest. The use of this technology is promising for the valorization of a by-product such as cambuci peel, which has not yet been widely studied and could contribute to the reduction of waste and would consequently favor the circular economy, a topic of great interest at present.

Finally, additional analyses, such as infrared (IR) spectroscopy for the identification of functional groups, mass spectrometry for identifying and quantifying compounds, or nuclear magnetic resonance (NMR), along with assessments for toxicity, microbiological activity, and stability of phenolic compounds, could be conducted. These analyses would provide detailed structural information about the compounds in this raw material and explore its potential applications across various industries.

Acknowledgements This study received support from Brazilian Science and Research Foundation (CNPq) (productivity grant 302451/2021-8 and 302610/2021-9) and São Paulo Research Foundation (FAPESP) number 2018/14938-4 (Tânia Forster Carneiro), 2018/14582-5 (Mauricio Ariel Rostagno), 2020/03623-2 (Letícia Sanches Contieri), 2022/11690-7 (Leonardo de Freitas Marinho), 2023/02064-8 (Tiago Linhares Cruz Tabosa Barroso), and 2023/04479-0 (Juver Andrey Jimenez Moreno). The authors thank the Multiuser Central Facilities (UFABC) for the experimental support.

Author Contributions J.A.J.M: Conceptualization, Methodology, Investigation, Validation, Writing - Original draft, Writing - review &; editing. L.F.M: Investigation, Validation, Writing - review &; editing. L.S.C: Validation, Writing - review &; editing. T.L.C.T.B: Validation, Writing - review &; editing. M.A.R: Supervision, Resources, Writing - review &; editing. T.F.C: Conceptualization, Methodology, Supervision, Resources, Project administration, Funding acquisition, Writing - review &; editing.

Funding This study received support from Brazilian Science and Research Foundation (CNPq) (productivity grant 302451/2021-8 and 302610/2021-9) and São Paulo Research Foundation (FAPESP) number 2018/14938-4 (Tânia Forster Carneiro), 2018/14582-5 (Mauricio Ariel Rostagno), 2020/03623-2 (Letícia Sanches Contieri), 2022/11690-7 (Leonardo de Freitas Marinho), 2023/02064-8 (Tiago Linhares Cruz Tabosa Barroso), and 2023/04479-0 (Juver Andrey Jimenez Moreno).

Data Availability No datasets were generated or analysed during the current study.

Declarations

Competing Interests The authors declare no competing interests.

References

Agcam, E. (2022). A kinetic approach to explain hydroxymethylfurfural and furfural formations induced by Maillard, caramelization, and ascorbic acid degradation reactions in fruit juice-based mediums. *Food Analytical Methods, 15*(5), 1286–1299. https://doi.org/10.1007/s12161-021-02214-x

Aguilar-Zárate, P., Wong-Paz, J. E., Michel, M., Buenrostro-Figueroa, J., Díaz, H. R., Ascacio, J. A., Contreras-Esquivel, J. C., Gutiérrez-Sánchez, G., & Aguilar, C. N. (2017). Characterisation of pomegranate-husk polyphenols and semi-preparative fractionation of punicalagin. *Phytochemical Analysis, 28*(5), 433–438. https://doi.org/10.1002/pca.2691

Ahmed, R., & Chun, B. S. (2018). Subcritical water hydrolysis for the production of bioactive peptides from tuna skin collagen. *The Journal of Supercritical Fluids, 141*, 88–96. https://doi.org/10.1016/J.SUPFLU.2018.03.006

Akter, S., Hong, H., Netzel, M., Tinggi, U., Fletcher, M., Osborne, S., & Sultanbawa, Y. (2021). Determination of ellagic acid, punicalagin, and castalagin from Terminalia ferdinandiana (Kakadu plum) by a validated UHPLC-PDA-MS/MS methodology. *Food Analytical Methods, 14*(12), 2534–2544. https://doi.org/10.1007/s12161-021-02063-8

Ali, M. C., Chen, J., Zhang, H., Li, Z., Zhao, L., & Qiu, H. (2019). Effective extraction of flavonoids from lycium barbarum L. fruits by deep eutectic solvents-based ultrasound-assisted extraction. *Talanta, 203*, 16–22. https://doi.org/10.1016/J.TALANTA.2019.05.012

Angonese, M., Motta, G. E., Silva de Farias, N., Molognoni, L., Daguer, H., Brugnerotto, P., de Oliveira Costa, A. C., & Olivera Müller, C. M. (2021). Organic dragon fruits (Hylocereus undatus and Hylocereus polyrhizus) grown at the same edaphoclimatic conditions: Comparison of phenolic and organic acids profiles and antioxidant activities. *LWT, 149*, 111924. https://doi.org/10.1016/J.LWT.2021.111924

AOAC. (2012). *Official methods of analysis of AOAC international* (19th ed.). Association of Official Analytical Chemistry, Arlington, VA. The USA.

Arslan, D., Steinbusch, K. J. J., Diels, L., Hamelers, H. V. M., Strik, D. P. B. T. B., Buisman, C. J. N., & de Wever, H. (2016). Selective short-chain carboxylates production: A review of control mechanisms to direct mixed culture fermentations. *Critical Reviews in Environmental Science and Technology, 46*(6), 592–634. https://doi.org/10.1080/10643389.2016.1145959

Barba, F. J., Parniakov, O., Pereira, S. A., Wiktor, A., Grimi, N., Boussetta, N., Saraiva, J. A., Raso, J., Martin-Belloso, O., Witrowa-Rajchert, D., Lebovka, N., & Vorobiev, E. (2015). Current applications and new opportunities for the use of pulsed electric fields in food science and industry. *Food Research International, 77*, 773–798. https://doi.org/10.1016/J.FOODRES.2015.09.015

Barbieri, S. F., Ruthes, A. C., de Petkowicz, C. L., & O., de Godoy, R. C. B., Sassaki, G. L., Santana Filho, A. P., & Silveira, J. L. M. (2017). Extraction, purification and structural characterization of a galactoglucomannan from the gabiroba fruit (Campomanesia xanthocarpa Berg), Myrtaceae family. *Carbohydrate Polymers, 174*, 887–895. https://doi.org/10.1016/J.CARBPOL.2017.07.015

Barros, L., Dueñas, M., Pinela, J., Carvalho, A. M., Buelga, C. S., & Ferreira, I. C. F. R. (2012). Characterization and quantification of phenolic compounds in four tomato (Lycopersicon esculentum L.) farmers' varieties in Northeastern Portugal homegardens. *Plant Foods for Human Nutrition, 67*(3), 229–234. https://doi.org/10.1007/s11130-012-0307-z

Barroso, T. L. C. T., da Rosa, R. G., Sganzerla, W. G., Castro, L. E. N., Maciel-Silva, F. W., Rostagno, M. A., & Forster-Carneiro, T. (2022a). Hydrothermal pretreatment based on semi-continuous flow-through sequential reactors for the recovery of bioproducts from jabuticaba (Myrciaria cauliflora) peel. *The Journal of Supercritical Fluids, 191*, 105766. https://doi.org/10.1016/J.SUPFLU.2022.105766

Barroso, T., Sganzerla, W., Rosa, R., Castro, L., Maciel-Silva, F., Rostagno, M., & Forster-Carneiro, T. (2022b). Semi-continuous flow-through hydrothermal pretreatment for the recovery of bioproducts from jabuticaba (Myrciaria cauliflora) agro-industrial by-product. *Food Research International, 158*, 111547. https://doi.org/10.1016/J.FOODRES.2022.111547

Benzie, I. F. F., & Strain, J. J. (1996). The ferric reducing ability of plasma (FRAP) as a measure of "antioxidant power": The FRAP assay. *Analytical Biochemistry, 239*(1), 70–76. https://doi.org/10.1006/ABIO.1996.0292

Bodoira, R., Velez, A., Rovetto, L., Ribotta, P., Maestri, D., & Martínez, M. (2019). Subcritical fluid extraction of antioxidant phenolic

compounds from pistachio (*Pistacia vera* L.) nuts: Experiments, modeling, and optimization. *Journal of Food Science, 84*(5), 963–970. https://doi.org/10.1111/1750-3841.14507

Bunmusik, W., Suttiarporn, P., Phankaew, T., Thitisut, P., & Seangwattana, T. (2022). The effects of solvent–based ultrasonic–assisted extraction of bioactive compounds and antioxidant activities from pigmented rice bran. *Materials Today: Proceedings*. https://doi.org/10.1016/J.MATPR.2022.11.391

Carocho, M., Barros, L., Bento, A., Santos-Buelga, C., Morales, P., & Ferreira, I. C. F. R. (2014). Castanea sativa Mill. flowers amongst the most powerful antioxidant matrices: A phytochemical approach in decoctions and infusions. *BioMed Research International, 2014*, 1–7. https://doi.org/10.1155/2014/232956

Castro, L. E. N., Sganzerla, W. G., Barroso, T. L. C. T., Maciel-Silva, F. W., Colpini, L. M. S., Bittencourt, P. R. S., Rostagno, M. A., & Forster-Carneiro, T. (2023). Improving the semi-continuous flow-through subcritical water hydrolysis of grape pomace (Vitis vinifera L) by pH and temperature control. *The Journal of Supercritical Fluids, 196*, 105894. https://doi.org/10.1016/j.supflu.2023.105894

Chanioti, S., & Tzia, C. (2018). Extraction of phenolic compounds from olive pomace by using natural deep eutectic solvents and innovative extraction techniques. *Innovative Food Science & Emerging Technologies, 48*, 228–239. https://doi.org/10.1016/J.IFSET.2018.07.001

Chen, Y., Pinegar, L., Immonen, J., & Powell, K. M. (2023). Conversion of food waste to renewable energy: A techno-economic and environmental assessment. *Journal of Cleaner Production, 385*, 135741. https://doi.org/10.1016/J.JCLEPRO.2022.135741

Cocero, M. J., Cabeza, Á., Abad, N., Adamovic, T., Vaquerizo, L., Martínez, C. M., & Pazo-Cepeda, M. V. (2018). Understanding biomass fractionation in subcritical & supercritical water. *The Journal of Supercritical Fluids, 133*, 550–565. https://doi.org/10.1016/J.SUPFLU.2017.08.012

Cvjetko Bubalo, M., Ćurko, N., Tomašević, M., Kovačević Ganić, K., & Radojcic Redovnikovic, I. (2016). Green extraction of grape skin phenolics by using deep eutectic solvents. *Food Chemistry, 200*, 159–166. https://doi.org/10.1016/J.FOODCHEM.2016.01.040

Da Silva, L. C., Viganó, J., Sanches, V. L., De Souza Mesquita, L. M., Pizani, R., & Rostagno, M. A. (2023). Simultaneous extraction and analysis of apple pomace by gradient pressurized liquid extraction coupled in-line with solid-phase extraction and on-line with HPLC. *Food Chemistry, 407*, 135117. https://doi.org/10.1016/j.foodchem.2022.135117

da Silveira, A. C., Kassuia, Y. S., Domahovski, R. C., & Lazzarotto, M. (2018). Método de DPPH adaptado: Uma ferramenta para analisar atividade antioxidante de polpa de frutos da erva-mate de forma rápida e reprodutível. In*Embrapa Florestas-Comunicado Técnico (INFOTECA-E); Comunicado Técnico (CNPF): Colombo*, Sri Lanka..

Damiani, C., de Vilas Boas, E. V., Asquieri, E. R., Lage, M. E., Oliveira, R. A., da Silva, F. A., Oliveira, D. M., Rodrigues, L. J., Silva, E. P., & de Paula, N. R. (2011). Characterization of fruits from the savanna: Araça (Psidium guinnensis Sw.) and Marolo (Annona crassiflora Mart.). *Ciência e Tecnologia de Alimentos, 31*(3), 723–729. https://doi.org/10.1590/S0101-20612011000300026

Donado-Pestana, C. M., Belchior, T., Festuccia, W. T., & Genovese, M. I. (2015). Phenolic compounds from cambuci (Campomanesia phaea O. Berg) fruit attenuate glucose intolerance and adipose tissue inflammation induced by a high-fat, high-sucrose diet. *Food Research International, 69*, 170–178. https://doi.org/10.1016/J.FOODRES.2014.12.032

Donado-Pestana, C. M., Moura, M. H. C., de Araujo, R. L., de Lima Santiago, G., de Moraes Barros, H. R., & Genovese, M. I. (2018). Polyphenols from Brazilian native Myrtaceae fruits and their potential health benefits against obesity and its associated complications. *Current Opinion in Food Science, 19*, 42–49. https://doi.org/10.1016/J.COFS.2018.01.001

Donado-Pestana, C. M., Pessoa, E. V. M., Rodrigues, L., Rossi, R., Moura, M. H. C., dos Santos-Donado, P. R., Castro, É., Festuccia, W. T., & Genovese, M. I. (2021). Polyphenols of cambuci (Campomanesia phaea (O. Berg.)) fruit ameliorate insulin resistance and hepatic steatosis in obese mice. *Food Chemistry, 340*, 128169. https://doi.org/10.1016/J.FOODCHEM.2020.128169

Farouk, A., Elbehery, H., Embaby, H., Abdel-aziz, N. F., Abd El-wahab, T., Abouamer, W., & Hussein, H. (2023). Phenolics from Nigella sativa L. straw: Characterization and insecticidal activity against Agrotis ipsilon (Hüfnagel). *Heliyon, 9*(12), e22995. https://doi.org/10.1016/j.heliyon.2023.e22995

Ferreira, V. C., Sganzerla, W. G., Barroso, T. L. C. T., Castro, L. E. N., Colpini, L. M. S., & Forster-Carneiro, T. (2023). Sustainable valorization of pitaya (Hylocereus spp.) peel in a semi-continuous high-pressure hydrothermal process to recover value-added products. *Food Research International, 173*, 113332. https://doi.org/10.1016/J.FOODRES.2023.113332

Gan, A., & Baroutian, S. (2022). Subcritical water extraction for recovery of phenolics and fucoidan from New Zealand Wakame (Undaria pinnatifida) seaweed. *The Journal of Supercritical Fluids, 190*, 105732. https://doi.org/10.1016/J.SUPFLU.2022.105732

García-Villalba, R., Espín, J. C., Aaby, K., Alasalvar, C., Heinonen, M., Jacobs, G., Voorspoels, S., Koivumäki, T., Kroon, P. A., Pelvan, E., Saha, S., & Tomás-Barberán, F. A. (2015). Validated method for the characterization and quantification of extractable and nonextractable ellagitannins after acid hydrolysis in pomegranate fruits, juices, and extracts. *Journal of Agricultural and Food Chemistry, 63*(29), 6555–6566. https://doi.org/10.1021/acs.jafc.5b02062

Gilchrist, A., & Nobbs, J. (2017). Colorimetry, theory. *Encyclopedia of Spectroscopy and Spectrometry*. https://doi.org/10.1016/B978-0-12-803224-4.00124-2

Giombelli, C., Iwassa, I. J., da Silva, C., & Bolanho Barros, B. C. (2020). Valorization of peach palm by-product through subcritical water extraction of soluble sugars and phenolic compounds. *The Journal of Supercritical Fluids, 165*, 104985. https://doi.org/10.1016/j.supflu.2020.104985

Grimaldi, M., Pitirollo, O., Ornaghi, P., Corradini, C., & Cavazza, A. (2022). Valorization of agro-industrial byproducts: Extraction and analytical characterization of valuable compounds for potential edible active packaging formulation. *Food Packaging and Shelf Life, 33*, 100900. https://doi.org/10.1016/J.FPSL.2022.100900

He, S., Zhang, Z., Sun, H., Zhu, Y., Zhao, J., Tang, M., Wu, X., & Cao, Y. (2019). Contributions of temperature and l-cysteine on the physicochemical properties and sensory characteristics of rapeseed flavor enhancer obtained from the rapeseed peptide and d-xylose Maillard reaction system. *Industrial Crops and Products, 128*, 455–463. https://doi.org/10.1016/J.INDCROP.2018.11.048

Herbst, G., Hamerski, F., Errico, M., Corazza, L., & M. (2021). Pressurized liquid extraction of brewer's spent grain: Kinetics and crude extracts characterization. *Journal of Industrial and Engineering Chemistry, 102*, 370–383. https://doi.org/10.1016/J.JIEC.2021.07.020

Jeong, Y. R., Park, J. S., Nkurunziza, D., Cho, Y. J., & Chun, B. S. (2021). Valorization of blue mussel for the recovery of free amino acids rich products by subcritical water hydrolysis. *The Journal of Supercritical Fluids, 169*, 105135. https://doi.org/10.1016/J.SUPFLU.2020.105135

Jha, A. K., & Sit, N. (2022). Extraction of bioactive compounds from plant materials using combination of various novel methods: A review. *Trends in Food Science & Technology, 119*, 579–591. https://doi.org/10.1016/J.TIFS.2021.11.019

Kumar, K., Srivastav, S., & Sharanagat, V. S. (2021). Ultrasound assisted extraction (UAE) of bioactive compounds from fruit and vegetable processing by-products: A review. *Ultrasonics Sonochemistry, 70*, 105325. https://doi.org/10.1016/J.ULTSONCH.2020.105325

Lachos-Perez, D., Baseggio, A. M., Torres-Mayanga, P. C., Ávila, P. F., Tompsett, G. A., Marostica, M., Goldbeck, R., Timko, M. T., Rostagno, M., Martinez, J., & Forster-Carneiro, T. (2020). Sequential subcritical water process applied to orange peel for the recovery flavanones and sugars. *The Journal of Supercritical Fluids, 160*, 104789. https://doi.org/10.1016/J.SUPFLU.2020.104789

Li, Q., Li, X., Ren, Z., Wang, R., Zhang, Y., Li, J., Ma, F., & Liu, X. (2021). Physicochemical properties and antioxidant activity of Maillard reaction products derived from Dioscorea opposita polysaccharides. *LWT, 149*, 111833. https://doi.org/10.1016/J.LWT.2021.111833

Maciel-Silva, F. W., Lachos-Perez, D., Buller, L. S., Sganzerla, W. G., Pérez, M., Rostagno, M. A., & Forster-Carneiro, T. (2022). Green extraction processes for complex samples from vegetable matrices coupled with on-line detection system: A critical review. *Molecules, 27*(19), 6272. https://doi.org/10.3390/molecules27196272

Maciel-Silva, F. W., Mussatto, S. I., & Forster-Carneiro, T. (2019). Integration of subcritical water pretreatment and anaerobic digestion technologies for valorization of açai processing industries residues. *Journal of Cleaner Production, 228*, 1131–1142. https://doi.org/10.1016/J.JCLEPRO.2019.04.362

Martins-Vieira, J. C., Torres-Mayanga, P. C., & Lachos-Perez, D. (2023). Hydrothermal processing of lignocellulosic biomass: An overview of subcritical and supercritical water hydrolysis. *BioEnergy Research, 16*(3), 1296–1317. https://doi.org/10.1007/s12155-022-10553-8

Mesquita, P. C., Rodrigues, L. G. G., Mazzutti, S., Ribeiro, P. R. V., de Brito, E. S., & Lanza, M. (2022). Untargeted metabolomic profile of recovered bioactive compounds by subcritical water extraction of acerola (Malpighia emarginata DC.) pomace. *Food Chemistry, 397*, 133718. https://doi.org/10.1016/j.foodchem.2022.133718

Murugan, A., Rubavathi, A., Kannan, V., & Parthiban, A. (2020). Bioconversion of mango pulp industrial waste into ellagic acid using Aspergillus niger. *BioRxiv*, 2020.03.17.996074. https://doi.org/10.1101/2020.03.17.996074

Murugesan, K., Srinivasan, K. R., Paramasivam, K., Selvam, A., & Wong, J. (2021). Conversion of food waste to animal feeds. *Current Developments in Biotechnology and Bioengineering: Sustainable Food Waste Management: Resource Recovery and Treatment*. https://doi.org/10.1016/B978-0-12-819148-4.00011-7

Nelson, N. (1944). A photometric adaptation of the Somogyi method for the determination of glucose. *Journal of Biological Chemistry, 153*(2), 375–380. https://doi.org/10.1016/S0021-9258(18)71980-7

Ohta, N., & Robertson, A. R. (2006). Color Vision and Color Specification Systems. In M.A. Kriss, N. Ohta, & A.R. Robertson (Eds), *Colorimetry*. https://doi.org/10.1002/0470094745.ch2

Oliveira, T. C. G., Hanlon, K. E., Interlandi, M. A., Torres-Mayanga, P. C., Silvello, M. A. C., Lachos-Perez, D., Timko, M. T., Rostagno, M. A., Goldbeck, R., & Forster-Carneiro, T. (2020). Subcritical water hydrolysis pretreatment of sugarcane bagasse to produce second generation ethanol. *The Journal of Supercritical Fluids, 164*, 104916. https://doi.org/10.1016/J.SUPFLU.2020.104916

Oliveira, V. B., Yamada, L. T., Fagg, C. W., & Brandão, M. G. L. (2012). Native foods from Brazilian biodiversity as a source of bioactive compounds. *Food Research International, 48*(1), 170–179. https://doi.org/10.1016/J.FOODRES.2012.03.011

Osamede Airouyuwa, J., Mostafa, H., Riaz, A., & Maqsood, S. (2022). Utilization of natural deep eutectic solvents and ultrasound-assisted extraction as green extraction technique for the recovery of bioactive compounds from date palm (Phoenix dactylifera L.) seeds: An investigation into optimization of process parameters. *Ultrasonics Sonochemistry, 91*, 106233. https://doi.org/10.1016/J.ULTSONCH.2022.106233

Özkaynak Kanmaz, E. (2018). 5-Hydroxymethylfurfural (HMF) formation during subcritical water extraction. *Food Science and Biotechnology, 27*(4), 981–986. https://doi.org/10.1007/s10068-018-0328-y

Paes, M. S., de Pessoa Filho, P., & Tadini, C. C. (2021). Sorption properties of cambuci (Campomanesia phaea O. Berg) untreated and pre-treated with sorbitol as osmotic solute. *LWT, 139*, 110569. https://doi.org/10.1016/J.LWT.2020.110569

Park, S. H., Kim, J.-H., Min, S.-G., Jo, Y.-J., & Chun, J.-Y. (2015). Effects of ethanol addition on the efficiency of subcritical water extraction of proteins and amino acids from porcine placenta. *Korean Journal for Food Science of Animal Resources, 35*(2), 265–271. https://doi.org/10.5851/kosfa.2015.35.2.265

Pattnaik, F., Nanda, S., Kumar, V., Naik, S., & Dalai, A. K. (2021). Subcritical water hydrolysis of Phragmites for sugar extraction and catalytic conversion to platform chemicals. *Biomass and Bioenergy, 145*, 105965. https://doi.org/10.1016/j.biombioe.2021.105965

Pińkowska, H., Krzywonos, M., Wolak, P., Seruga, P., Górniak, A., Złocińska, A., & Ptak, M. (2020). Sustainable production of 5-hydroxymethylfurfural from pectin-free sugar beet pulp in a simple aqueous phase system-optimization with Doehlert design. *Energies, 13*(21), 5649. https://doi.org/10.3390/en13215649

Pinto, D., Vieira, E. F., Peixoto, A. F., Freire, C., Freitas, V., Costa, P., Delerue-Matos, C., & Rodrigues, F. (2021). Optimizing the extraction of phenolic antioxidants from chestnut shells by subcritical water extraction using response surface methodology. *Food Chemistry, 334*, 127521. https://doi.org/10.1016/J.FOODCHEM.2020.127521

Rahmani, M., Azadbakht, M., Dastar, B., & Esmaeilzadeh, E. (2022). Production of animal feed from food waste or corn? Analyses of energy and exergy. *Bioresource Technology Reports, 20*, 101213. https://doi.org/10.1016/J.BITEB.2022.101213

Rojas-González, A. F., Flórez-Montes, C., & López-Rodríguez, D. F. (2019). Use prospects of some agroindustrial waste. *Revista Cubana De Química, 31*(1), 31–52.

Saldanha, L., Vilegas, W., & Dokkedal, A. (2013). Characterization of flavonoids and phenolic acids in Myrcia bella Cambess. Using FIA-ESI-IT-MSn and HPLC-PAD-ESI-IT-MS combined with NMR. *Molecules, 18*(7), 8402–8416. https://doi.org/10.3390/molecules18078402

Sanches, M. C. R. (2013). *Caracterização do fruto de cambuci (Campomanesia phaea O. Berg.) e efeito da destanização sobre o potencial funcional in vitro* Masters dissertation, Faculdade de Ciências Farmacêuticas, Universidade de São Paulo, São Paulo. https://doi.org/10.11606/D.9.2013.tde-01082013-111601

Sanches Azevedo, M. C., Silva, R. R. E., Jacomino, A. P., & Genovese, M. I. (2017). Physicochemical variability of cambuci fruit (Campomanesia phaea) from the same orchard, from different locations and at different ripening stages. *Journal of the Science of Food and Agriculture, 97*(2), 526–535. https://doi.org/10.1002/jsfa.7756

Schiassi, M. C. E. V., de Souza, V. R., Lago, A. M. T., Campos, L. G., & Queiroz, F. (2018). Fruits from the Brazilian Cerrado region: Physico-chemical characterization, bioactive compounds, antioxidant activities, and sensory evaluation. *Food Chemistry, 245*, 305–311. https://doi.org/10.1016/j.foodchem.2017.10.104

Seraglio, S. K. T., Schulz, M., Nehring, P., Della Betta, F., Valese, A. C., Daguer, H., Gonzaga, L. V., Fett, R., & Costa, A. C. O. (2018). Nutritional and bioactive potential of Myrtaceae fruits during ripening. *Food Chemistry, 239*, 649–656. https://doi.org/10.1016/J.FOODCHEM.2017.06.118

Sganzerla, W. G., Viganó, J., Castro, L. E. N., Maciel-Silva, F. W., Rostagno, M. A., Mussatto, S. I., & Forster-Carneiro, T. (2022).

Recovery of sugars and amino acids from brewers' spent grains using subcritical water hydrolysis in a single and two sequential semi-continuous flow-through reactors. *Food Research International, 157*, 111470. https://doi.org/10.1016/J.FOODRES.2022.111470

Singh, P. P., & Saldaña, M. D. A. (2011). Subcritical water extraction of phenolic compounds from potato peel. *Food Research International, 44*(8), 2452–2458. https://doi.org/10.1016/J.FOODRES.2011.02.006

Singleton, V. L., Orthofer, R., & Lamuela-Raventós, R. M. (1999). [14] Analysis of total phenols and other oxidation substrates and antioxidants by means of Folin-Ciocalteu reagent. *Methods in Enzymology, 299*, 152–178. https://doi.org/10.1016/S0076-6879(99)99017-1

Song, R., Ismail, M., Baroutian, S., & Farid, M. (2018). Effect of subcritical water on the extraction of bioactive compounds from carrot leaves. *Food and Bioprocess Technology, 11*(10), 1895–1903. https://doi.org/10.1007/s11947-018-2151-0

Souza Ronchi, H. (2021). *Cadeia produtiva dos frutos da Campomanesia phaea (cambuci): Prospecção de produtos medicinais, aromáticos e alimentícios e sua inserção no mercado*. Universidade Estadual Paulista "Júlio de Mesquita Filho", São Paulo.

Stefanello, M. É. A., Pascoal, A. C. R. F., & Salvador, M. J. (2011). Essential oils from neotropical Myrtaceae: Chemical diversity and biological properties. *Chemistry & Biodiversity, 8*(1), 73–94. https://doi.org/10.1002/cbdv.201000098

Tokairin, T. D., Silva, A. P., Spricigo, P. C., Alencar, S. M., & Jacomino, A. P. (2018). Cambuci: A native fruit from the Brazilian Atlantic forest showed nutraceutical characteristics. *Revista Brasileira de Fruticultura*. https://doi.org/10.1590/0100-29452018666

Vedovatto, F., Ugalde, G., Bonatto, C., Bazoti, S. F., Treichel, H., Mazutti, M. A., Zabot, G. L., & Tres, M. V. (2021). Subcritical water hydrolysis of soybean residues for obtaining fermentable sugars. *The Journal of Supercritical Fluids, 167*, 105043. https://doi.org/10.1016/J.SUPFLU.2020.105043

Yao, G. Y., Chen, X. P., Long, Z. Y., Du, X. B., Liang, J. Z., Wei, X. J., & Wang, L. L. (2023). The non-enzymatic browning of pine bark during thermal treatment: Color and chemical changes, color kinetics and insights into mechanisms. *Industrial Crops and Products, 204*, 117289. https://doi.org/10.1016/J.INDCROP.2023.117289

Yee, L. K., & A., Razali, M., Ismail, M. A. M., Yusoff, I. N., Nagendran, S. K., Zainal, Z., Tobe, H., Date, K., & Yokota, Y. (2023). Preliminary analysis of rock mass weathering grade using image analysis of CIELAB color space with the validation of Schmidt hammer: A case study. *Physics and Chemistry of the Earth, Parts A/B/C, 129*, 103291. https://doi.org/10.1016/j.pce.2022.103291

Yeo, J., & Shahidi, F. (2019). Critical re-evaluation of DPPH assay: Presence of pigments affects the results. *Journal of Agricultural and Food Chemistry, 67*(26), 7526–7529. https://doi.org/10.1021/acs.jafc.9b02462

Zhang, J., Wen, C., Zhang, H., Duan, Y., & Ma, H. (2020). Recent advances in the extraction of bioactive compounds with subcritical water: A review. *Trends in Food Science & Technology, 95*, 183–195. https://doi.org/10.1016/j.tifs.2019.11.018